

# 1 **Membrane-Interactive Compounds from *Pistacia lentiscus* L.** 2 **Thwart *Pseudomonas aeruginosa* Virulence**

3  
4 **Ali Tahrioui<sup>#,1</sup>, Sergio Ortiz<sup>2</sup>, Onyedikachi Cecil Azuama<sup>1</sup>, Emeline Bouffartigues<sup>1</sup>,**  
5 **Nabiha Benalia<sup>2</sup>, Damien Tortuel<sup>1</sup>, Olivier Maillot<sup>1</sup>, Smain Chemat<sup>3</sup>, Marina Kritsanida<sup>2</sup>,**  
6 **Marc Feuilloley<sup>1</sup>, Nicole Orange<sup>1</sup>, Sylvie Michel<sup>2</sup>, Olivier Lesouhaitier<sup>1</sup>, Pierre Cornelis<sup>1</sup>,**  
7 **Raphaël Grougnet<sup>2</sup>, Sabrina Boutefnouchet<sup>2</sup> & Sylvie Chevalier<sup>1</sup>**

8  
9  
10 <sup>1</sup>Université de Rouen Normandie, Normandie Université, Laboratoire de Microbiologie  
11 Signaux et Microenvironnement, LMSM EA4312, Évreux, France

12 <sup>2</sup>Université Paris Descartes, Faculté des Sciences Pharmaceutiques et Biologiques, Équipe  
13 Produits Naturels, Analyses et Synthèses (PNAS), CiTCoM UMR 8038 CNRS, Paris, France

14 <sup>3</sup>Centre de Recherche Scientifique et Technique en Analyses Physico-Chimiques, CRAPC,  
15 Bou Ismaïl, Algérie

16  
17  
18 #Corresponding author:

19 Dr. Ali Tahrioui

20 Laboratory of Microbiology Signals and Microenvironment–LMSM EA4312, University of  
21 Rouen Normandy–Normandy University, 55 Rue Saint-Germain, 27000 Evreux, France

22 E-mail: [ali.tahrioui@univ-rouen.fr](mailto:ali.tahrioui@univ-rouen.fr)

23 Phone: (+33) 2.32.29.15.60

24 Fax: (+33) 2.32.29.15.50

25  
26 Running Title: *Pistacia lentiscus* L. fruit prevents *Pseudomonas aeruginosa* virulence

27 Keywords: *Pistacia lentiscus*, Fruit-derived extract, Ginkgolic acids, Anti-virulence,  
28 *Pseudomonas aeruginosa*, Membrane stiffness, ECF $\sigma$  SigX

30 **ABSTRACT**

31 *Pseudomonas aeruginosa* is capable to deploy a collection of virulence factors that are not  
32 only essential for host infection and persistence, but also to escape from the host immune  
33 system and to become more resistant to drug therapies. Thus, developing anti-virulence agents  
34 that may directly counteract with specific virulence factors or disturb higher regulatory  
35 pathways controlling the production of virulence armories are urgently needed. In this regard,  
36 this study reports that *Pistacia lentiscus* L. fruit cyclohexane extract (PLFE1) thwarts *P.*  
37 *aeruginosa* virulence by targeting mainly the pyocyanin pigment production by interfering with  
38 4-hydroxy-2-alkylquinolines molecules production. Importantly, the anti-virulence activity of  
39 PLFE1 appears to be associated with membrane homeostasis alteration through the  
40 modulation of SigX, an extracytoplasmic function sigma factor involved in cell wall stress  
41 response. A thorough chemical analysis of PLFE1 allowed us to identify the ginkgolic acid  
42 (C17:1) and hydroginkgolic acid (C15:0) as the main bioactive membrane-interactive  
43 compounds responsible for the observed increased membrane stiffness and anti-virulence  
44 activity against *P. aeruginosa*. This study delivers a promising perspective for the potential  
45 future use of PLFE1 or ginkgolic acid molecules as an adjuvant therapy to fight against *P.*  
46 *aeruginosa* infections.

47

## 48 INTRODUCTION

49 Bacterial infections still constitute a serious public health threat even though their prevention  
50 and treatment have been improved over the last decades. The effects of common antibiotics  
51 are no longer effective against microbial threats including *Enterococcus faecium*,  
52 *Staphylococcus aureus*, *Acinetobacter baumannii*, *Pseudomonas aeruginosa*, and  
53 *Enterobacter* species, also known as the “ESKAPE” pathogens group.<sup>1</sup> In a recent report  
54 published by the World Health Organization (WHO), *P. aeruginosa* was categorized as one of  
55 the “critical priority pathogens” for which there is an urgent need for the discovery of alternative  
56 and innovative new therapies.<sup>2</sup>

57

58 *P. aeruginosa* is predominantly responsible for different life-threatening infections in humans,  
59 including the respiratory system, burn and wound, urinary tract as well as medical implant  
60 devices.<sup>3</sup> This notorious multidrug resistant opportunistic Gram-negative bacterium deploys a  
61 wide variety of virulence factors and host-degrading enzymes as well as multiple secondary  
62 metabolites.<sup>4</sup> Pyocyanin is an important virulence factor produced and secreted abundantly by  
63 nearly 95% of *P. aeruginosa* isolates.<sup>5</sup> This phenazine-derived pigment, blue-green in color,  
64 confers a greenish hue to the sputum of cystic fibrosis (CF) individuals suffering *P. aeruginosa*  
65 chronic lung infection.<sup>6</sup> Moreover, pyocyanin is a highly diffusible redox-active secondary  
66 metabolite which plays an important role in several physiological processes<sup>6,7</sup> making it a good  
67 target. Therefore, pyocyanin production hindrance may have consequences regarding the  
68 cytotoxic effects and the full virulence of *P. aeruginosa* during infections related to airways in  
69 CF.

70

71 The sophisticated quorum sensing (QS) circuitry in *P. aeruginosa* strongly controls the  
72 biosynthesis of pyocyanin. This process starts with the synthesis of the *N*-acyl-L-homoserine  
73 lactone (AHL) type signal molecules followed by the *Pseudomonas* quinolone signaling (PQS).  
74 Next, PQS regulates the expression of *phzA-G* operons resulting in the production of  
75 phenazine-1-carboxylic acid (PCA) which is then modified to produce predominantly pyocyanin  
76 *via* the action of the enzymes encoded by *phzM* and *phzS*.<sup>8</sup> In addition, pyocyanin biosynthesis  
77 and regulation have been also linked to SigX, an extracytoplasmic function sigma factor  
78 (ECF $\sigma$ ) that plays an essential role in the cell wall stress response network.<sup>9-12</sup> In *P.*  
79 *aeruginosa*, the ECF $\sigma$  SigX is a global regulator that modulates the expression of more than  
80 300 genes, including several genes involved in pyocyanin biosynthetic pathways.<sup>9,11,13</sup> More  
81 importantly, SigX has been reported to be involved in the regulation of fatty acid biosynthesis,  
82 which triggers changes in cell membrane phospholipid composition that affect membrane  
83 fluidity and envelope integrity.<sup>11,14-16</sup> SigX is also involved in physiological processes as  
84 important as iron uptake, virulence, motility, attachment, biofilm formation, and antibiotic  
85 resistance and susceptibility *via* direct and/or indirect governance.<sup>9-11,17</sup>

86  
87 In view of this, developing anti-virulence agents that may precisely hinder the production,  
88 secretion, or function of virulence determinants or interfere with their regulation has emerged  
89 as an alternative promising strategy to fight against bacterial pathogens.<sup>18,19</sup> Plants have long  
90 been used in traditional medicine to prevent or treat infectious diseases in many countries.<sup>20</sup>  
91 Hydrophilic and lipophilic extracts from plants were reported to contain abundant and diverse  
92 range of bioactive compounds with anti-virulence properties.<sup>19,21,22</sup> *Pistacia lentiscus* L., a plant  
93 commonly known as mastic tree or lentisc, is an evergreen shrub of the family of  
94 *Anacardiaceae* widespread all around the Mediterranean area where it grows wild in a variety  
95 of ecosystems.<sup>23,24</sup> Medicinal uses of the fruit, galls, resin, and leaves of *P. lentiscus* L. are

96 described since antiquity. However, they may differ either in the therapeutic indication or in the  
97 plant part used for medicinal purpose, depending of the geographical area.<sup>25,26</sup>

98

99 Currently, there are no research, which have explored the anti-virulence potential of *P.*  
100 *lentiscus* L. fruit, or the molecular mechanism of action, which underpins its major bioactive  
101 compounds against *P. aeruginosa*. Herein, we report that *P. lentiscus* L. fruit cyclohexane  
102 extract (PLFE1) can function as a potent pyocyanin inhibitor while being devoid of any  
103 antibacterial activity as judged by cell growth and viability assays. We show that PLFE1  
104 interferes with 4-hydroxy-2-alkylquinolines molecules production, which might explain its anti-  
105 pyocyanin activity. We also demonstrate that PLFE1 is able to increase significantly membrane  
106 stiffness in *P. aeruginosa*. Interestingly, the cell wall stress response ECF $\sigma$  SigX is found to be  
107 a key regulatory element in this phenomenon, which might respond to the presence of  
108 envelope-interactive compounds in PLFE1. Furthermore, comprehensive chemical analyses of  
109 PLFE1 and its derived fractions allowed us to identify the ginkgolic acid (C17:1) and  
110 hydroginkgolic acid (C15:0) as the major bioactive compounds and we confirmed that they are  
111 responsible of the main anti-virulence activity against the pathogen *P. aeruginosa*.

112

## 113 **RESULTS**

### 114 **Pyocyanin production inhibition by *P. lentiscus* L. fruit extracts**

115 Planktonic cultures of wild-type *P. aeruginosa* H103 were exposed to cyclohexane, ethyl  
116 acetate, methanol, and water *P. lentiscus* L. fruit extracts at concentrations of 100, 50, 25, 12.5,  
117 6.25, 3.12, 1.6 and 0.8  $\mu\text{g mL}^{-1}$  and assayed for interference with pyocyanin production (Fig.  
118 1A). Pyocyanin levels from H103 strain cultures untreated with *P. lentiscus* L. fruit extracts and  
119 treated with 1% v/v DMSO were also measured as negative control and defined as 100%

120 pyocyanin production. The PLFE1 (cyclohexane extract) showed statistically significant  
121 inhibition of pyocyanin biosynthesis at the all concentration tested. The PLFE1 at 100  $\mu\text{g mL}^{-1}$   
122 concentration caused the maximum percent reduction in pyocyanin production (82%;  
123  $P<0.0001$ ) over the untreated control with an  $\text{IC}_{50}$  value of 4.9  $\mu\text{g mL}^{-1}$ . In addition, PLFE1  
124 inhibitory activity was shown to be dose-dependent. The PLFE2 (ethyl acetate extract) was  
125 also capable of inhibiting pyocyanin biosynthesis following the same pattern as observed for  
126 PLFE1 but not in a drastic manner where approximately 50% of inhibition of this pigment  
127 production was observed at 100  $\mu\text{g mL}^{-1}$  ( $P<0.001$ ). There was no significant or slight variation  
128 in pyocyanin production by H103 strain when exposed to PLFE3 (methanol extract) or PLFE4  
129 (water extract). Of all the *P. lentiscus* L. fruit extracts tested for pyocyanin inhibition, PLFE1  
130 cyclohexane extract showed remarkably better inhibitory activity and was therefore selected  
131 for all further sets of experiments. Further, the inhibitory activity of PLFE1 on phenazine  
132 biosynthetic pathway was investigated at the level of gene expression. In the presence of  
133 PLFE1 at 100  $\mu\text{g mL}^{-1}$ , RT-qPCR analyses results showed significant down-regulation of the  
134 *phzA* gene involved in the production of phenazine-1-carboxylic acid (PCA), *phzM*, and *phzS*  
135 which converts PCA into the derivative pyocyanin (Fig. 1B). However, the expression levels of  
136 the *phzH* gene were not significantly different in H103 strain treated with PLFE1 as compared  
137 to untreated H103 (Fig. 1B). In summary, the repression of the expression levels of genes  
138 involved in phenazine biosynthesis correlate with pyocyanin production inhibition indicating that  
139 PLFE1 has the ability to function as a strong inhibitor of the pyocyanin virulence factor in *P.*  
140 *aeruginosa* H103 strain.

141

#### 142 ***P. aeruginosa* virulence attenuation by PLFE1**

143 We next sought to evaluate anti-virulence effect of PLFE1 on *P. aeruginosa* strain H103 using  
144 human lung A549 cells and *Caenorhabditis elegans* infection models. As depicted in Fig. 2A,

145 the results showed lower LDH release (20%;  $P \leq 0.05$ ) in A549 cells after their infection with  
146 H103 treated with PLFE1 ( $100 \mu\text{g mL}^{-1}$ ) for 20h incubation. A549 cells infected with non-treated  
147 strain H103 were used as a control. This result revealed that PLFE1 exhibited significant *P.*  
148 *aeruginosa* anti-virulence effect in human lung A549 cells. In addition, the impact of PLFE1 on  
149 *in vivo* virulence of *P. aeruginosa* strain H103 was assessed using a *C. elegans* fast-killing  
150 infection assay. When *C. elegans* worms were placed on a lawn of H103 strain, the percentage  
151 of nematodes survival drastically decreased (65%;  $P < 0.0001$ ) after 24h incubation as  
152 compared to *C. elegans* fed with *E. coli* OP50 (Fig. 2B). Interestingly, the presence of PLFE1  
153 ( $100 \mu\text{g mL}^{-1}$ ) significantly protected *C. elegans* from killing by *P. aeruginosa* (27%;  $P < 0.0001$ )  
154 as compared to *C. elegans* when applied to lawns of untreated H103 (Fig. 2B). Altogether,  
155 these data indicate that PLFE1 attenuated the virulence of *P. aeruginosa* strain H103 in human  
156 lung A549 cells and *C. elegans* infection models.

157

### 158 **Absence of effect of PLFE1 on *P. aeruginosa* growth and cell viability**

159 The impact of PLFE1 (cyclohexane extract) on the cell growth of *P. aeruginosa* H103 was  
160 monitored at 37 °C over the course of 24 h. None of the concentrations assayed (100, 50, 25,  
161 12.5, 6.25, 3.12, 1.6 and  $0.8 \mu\text{g mL}^{-1}$ ) had an impact on planktonic cell growth of H103 strain  
162 as compared to the untreated culture (H103 strain grown in presence of 1 % v/v DMSO)  
163 (Supplementary Fig. S1A). Moreover, the effect of PLFE1 on H103 cell viability was evaluated  
164 by flow cytometry using BacLight live/dead stain. Similarly, the results showed that at all the  
165 concentrations tested, PLFE1 did not affect the cell viability according to normalized events  
166 counting of live, injured, and dead cells when compared to the control condition  
167 (Supplementary Table S1 and Fig. S1B). Based on these results, it can be concluded that the  
168 inhibition of pyocyanin pigment production by *P. lentiscus* L. fruit extract (PLFE1) was achieved  
169 without affecting the growth of the bacteria and cell viability, at least *in vitro*.

170  
171  
172  
173  
174  
175  
176  
177  
178  
179  
180  
181  
182  
183  
184  
185  
186  
187  
188  
189  
190  
191  
192  
193

**PLFE1 modulates the production of 4-hydroxy-2-alkylquinolines (HAQs) molecules**

We next sought to assess whether the inhibition of pyocyanin production was directly due to PLFE1 on Pqs QS system that is known to tightly regulate pyocyanin biosynthesis. *P. aeruginosa* H103 cultures were exposed to different concentrations of PLFE1 (100, 50, 25, 12.5, 6.25, 3.12, 1.6 and 0.8  $\mu\text{g mL}^{-1}$ ) and then HAQs molecules were extracted twice by ethyl acetate. The production of HAQs was determined using a PAO1  $\Delta pqsA$  CTX-*pqsA::lux* biosensor strain which does not produce HAQs molecules and shows response to exogenous HAQs. The H103 cultures treated with 100, 50, and 25  $\mu\text{g mL}^{-1}$  of PLFE1 showed significant reduced HAQs production (Fig. 3A). Additionally, we measured the expression levels of *pqsA*, *pqsH*, *pqsL*, and *pqsR* genes representative of Pqs QS system by using RT-qPCR. The assays were performed after 24h of growth of H103 untreated or treated with 100, 25, and 6.25  $\mu\text{g mL}^{-1}$  PLFE1 (Fig. 3B). The *pqsA*, *pqsH* and *pqsL* genes involved in the biosynthesis of the major molecules from the HAQs family, namely 3,4-dihydroxy-2-heptylquinoline [termed the *Pseudomonas* quinolone signal (PQS)], its precursor 4-hydroxy-2-heptylquinoline (HHQ) and 4-hydroxy-2-heptylquinoline *N*-oxide (HQNO) were all significantly repressed upon exposure to PLFE1 at 100 and 25  $\mu\text{g mL}^{-1}$ . However, the expression of *pqsR* (*mvfR*) encoding for the cognate receptor/regulator of HHQ and PQS molecules did not change in the presence of 100 and 25  $\mu\text{g mL}^{-1}$  PLFE1. Taken together, these data indicate that PLFE1 extract represses gene expression levels of the Pqs QS system that correlates with the reduction in HAQs molecules production, suggesting that PLFE1 exhibits its anti-pyocyanin production effect possibly through an anti-QS activity.



194 **PLFE1 leads to increased membrane stiffness**

195 Further, we evaluated the effect of PLFE1 on *P. aeruginosa* strain H103 membrane fluidity  
196 homeostasis. Planktonic cell growths of H103 exposed to PLFE1 at concentrations of 100, 50,  
197 25, 12.5, 6.25, 3.12, 1.6 and 0.8  $\mu\text{g mL}^{-1}$  were assayed for fluorescence anisotropy (FA) using  
198 1,6-diphenyl-1,3,5-hexatriene (DPH) fluorescent probe (Fig. 4A). Anisotropy of H103 cells  
199 increased in a concentration dependent-manner to achieve a maximum FA value of  $0.223 \pm$   
200  $0.003$  ( $P < 0.001$ ) at a concentration of  $100 \mu\text{g mL}^{-1}$  of PLFE1 in comparison to the FA value of  
201 untreated control ( $0.186 \pm 0.002$ ). This result reflects a significant decrease of approximately  
202 20% of membrane fluidity (membrane rigidification) revealing physiological changes and  
203 adaptations in the cellular envelope of H103 in response to PLFE1 exposure. Interestingly,  
204 mRNA expression levels of *sigX* encoding the extracytoplasmic function sigma factor (ECF $\sigma$ )  
205 SigX that is required to maintain cell envelope integrity, and its known representative targets  
206 *accA*, *accB*, and *fabY* that are involved in fatty acid biosynthesis were significantly decreased  
207 upon exposure of H103 strain to PLFE1 at 100 and  $25 \mu\text{g mL}^{-1}$  when compared to mRNA  
208 expression levels in the control condition (untreated H103) (Fig. 4B). Further, *sigX* expression  
209 was monitored during growth in the presence of PLFE1 at 100, 25 and  $6.25 \mu\text{g mL}^{-1}$  by using  
210 a transcriptional fusion construction where the *sigX* promoter region was fused to the promoter-  
211 less *luxCDABE* cassette in the replicative pAB133 vector (pAB-P*sigX*) (Supplementary Fig.  
212 S2). Remarkably, in the presence of PLFE1, the relative bioluminescence output from H103  
213 harbouring pAB-P*sigX* increased in a dose dependent-manner reaching significant maximal  
214 activity at  $100 \mu\text{g mL}^{-1}$  during the transition from the late exponential phase to early stationary  
215 phase (Fig. 4C; Supplementary Fig. S2A). However, bioluminescence activity of pAB-P*sigX*  
216 decreased significantly in a concentration dependent-manner during the late stationary phase  
217 achieving minimal activity at  $100 \mu\text{g mL}^{-1}$  of PLFE1 (Fig. 4C; Supplementary Fig. S2A), in line  
218 with the RT-qPCR results presented in Fig. 4B. These results reveal that *P. aeruginosa*

219 exposure to PLFE1 induced increased membrane stiffness suggesting alterations in envelope  
220 homeostasis most likely through the activation of the cell wall stress ECF $\sigma$  SigX. To further  
221 validate this hypothesis, we used a  $\Delta sigX$  deletion mutant<sup>27</sup> to determine the FA in the absence  
222 or presence of various concentrations of PLFE1. The FA values appeared to be unaffected in  
223  $\Delta sigX$  in response to PLFE1 exposure compared to the control condition (untreated  $\Delta sigX$ )  
224 (Supplementary Fig. S2A). Altogether, these data indicate that PLFE1 contains bioactive  
225 membrane-interactive compounds that reduce membrane fluidity, in which the ECF $\sigma$  SigX  
226 seems to play a key role.

## 227

### 228 **Isolation and identification of major bioactive compounds of PLFE1**

229 To isolate and identify the major constituents of PLFE1, multiple chemical analyses were  
230 performed. The fractionation of PLFE1 by medium pressure liquid chromatography (MPLC)  
231 allowed to recover a total of 13 fractions that we labelled as PLFE1-(1-13) (Supplementary  
232 Table S2). Thin layer chromatography (TLC) examination showed that the major compounds  
233 of PLFE1 were present in the fractions PLFE1-(2-4). These last were then selected for further  
234 analyses in order to identify the main compounds present in each fraction. For PLFE1-2, <sup>1</sup>H-  
235 NMR spectra, proton signals between 7.36 and 6.78 ppm showed the presence of a tri-  
236 substituted aromatic ring. The signal at 5.36 ppm [ $t J = 4.6$  Hz, 2H] accounted for an olefinic  
237 double bond. The major derivative ginkgolic acid (C17:1) with a molecular formula of C<sub>24</sub>H<sub>38</sub>O<sub>3</sub>  
238 ( $m/z$  373.1 [M-H]<sup>-</sup>) displayed one unsaturation in its aliphatic chain. Ozonolysis reaction of  
239 PLFE1-2 allowed to localize the double bond of ginkgolic acid (C17:1) between positions C-8'  
240 and C-9' (Fig. 5). LC-ESI-MS analyses corroborated the presence of ginkgolic acid (C17:1) in  
241 PLFE1-2 and showed the occurrence of hydroginkgolic acid (C15:0) derivative and a mixture  
242 of both ginkgolic acids (C17:1/C15:0) in PLFE1-3 and PLFE1-4, respectively (Fig. 5).  
243 Altogether, these results indicate that ginkgolic acid (C17:1) and hydroginkgolic acid (C15:0)

244 are the main metabolites in PLFE1 and might be responsible for *P. aeruginosa* virulence  
245 attenuation.

246

### 247 **Ginkgolic acid-enriched fractions from PLFE1 are involved in virulence** 248 **attenuation of *P. aeruginosa***

249 To further assay whether GA (C17:1), GA (15:1) or a mixture of both GA (C17:1/C15:0) are the  
250 main bioactive compounds involved in the anti-virulence activity against *P. aeruginosa*, their  
251 effect on pyocyanin production and virulence attenuation in human lung A549 infection model  
252 was evaluated. Consistent with the results of pyocyanin inhibition by the crude extract PLFE1,  
253 H103 strain treated with GA-enriched fractions showed a dose-dependent reduction of  
254 pyocyanin production when compared to untreated H103 (Fig. 6A). Interestingly, the fractions  
255 enriched in GA (C17:1) or GA mix of (C17:1)/(C15:0) showed approximately 90% pyocyanin  
256 inhibition activity at 100  $\mu\text{g mL}^{-1}$ . The GA (C17:1) and GA (C15:0) displayed an  $\text{IC}_{50}$  of 6.3  $\mu\text{g}$   
257  $\text{mL}^{-1}$  (16.75  $\mu\text{M}$ ) and 12.5  $\mu\text{g mL}^{-1}$  (35.75  $\mu\text{M}$ ), respectively (Supplementary Fig. S3). Looking  
258 at virulence attenuation, H103 strain exposed to GA-enriched fractions showed significant  
259 reduced LDH release (20%) as compared to the control condition (H103 untreated) revealing  
260 that GA-enriched fractions were able to protect the human lung A549 line cells (Fig. 6B). Taken  
261 together, these results provide important insights into the involvement of GA-enriched fractions  
262 on the anti-virulence activity against *P. aeruginosa*.

263

### 264 **Cytotoxicity of PLFE1 and GA-enriched fractions**

265 Our last goal for this study was to investigate the potential of PLFE1 and its GA-enriched  
266 fractions to induce cytotoxicity in the human lung A549 cells. As depicted in Fig. 7A, no  
267 significant differences in cytotoxicity levels were found between A549 cells treated at various  
268 concentrations of crude extract PLFE1 after 1 h incubation as compared to the control condition

269 (untreated A549 cells). However, a moderate cytotoxic effect was observed when A549 cells  
270 were incubated for more than 3 h in the presence of PLFE1 at concentrations above 12.5  $\mu\text{g}$   
271  $\text{mL}^{-1}$ . Remarkably, when A549 cells were treated with PLFE1 at  $\text{IC}_{50}$  value of pyocyanin activity  
272 inhibition (4.9  $\mu\text{g mL}^{-1}$ ) there was no differences in cytotoxicity at different time points incubation  
273 assayed (1 h, 3 h, 6 h, and 24 h) (Fig. 7B). Moreover, similar interesting trend results were  
274 obtained for the GA-enriched fraction mix of both GA (C17:1/C15:0) when tested at 5.4  $\mu\text{g mL}^{-1}$   
275  $\text{IC}_{50}$  value of pyocyanin inhibition (Fig. 7B). On the other hand, after 3 h incubation, a slight  
276 cytotoxicity increase was observed when A549 cells were exposed to enriched fractions of GA  
277 (C17:1) and GA (C15:0) separately at their  $\text{IC}_{50}$  values (6.3  $\mu\text{g mL}^{-1}$  and 12.5  $\mu\text{g mL}^{-1}$ ,  
278 respectively) (Fig. 7B). However, this cytotoxicity increased by about 3-fold after 24 h exposure  
279 as compared to the control condition (A549 cells treated with DMSO). In summary, these  
280 results indicate that PLFE1 and its complex GA-enriched fraction (C17:1/C15:0) displayed no  
281 significant cytotoxicity in the human lung A549 line cells when tested at their  $\text{IC}_{50}$  pyocyanin  
282 inhibition values.

283

284

## 285 DISCUSSION

286 Antibiotic-resistant pathogens are threatening individuals and public health over the world to a  
287 such extent that new therapeutic strategies need to be developed urgently.<sup>2,18</sup> The anti-  
288 virulence approaches represent an attracting alternative to the unmet clinical need in the  
289 treatment of bacterial infections.<sup>28,29</sup> These new therapies target essentially the prevention of  
290 virulence factors production by pathogens, rather than their survival, and they also aim to thwart  
291 the regulatory mechanisms controlling their expression.<sup>19,30</sup> In addition, by targeting essential  
292 virulence determinants, the emergence and spread of bacterial resistance will be reduced due  
293 to decreased selective pressure and the natural microbiota will be preserved. In line with this  
294 scenario, the current study was designed to explore new anti-virulence agents to fight against  
295 the multidrug-resistant *P. aeruginosa* that is responsible for many different infections. Thus, we  
296 based our research on the traditional medicine reported to treat several infectious diseases. In  
297 particular, the fruit of *P. lentiscus* L. is used for the treatment of respiratory tracts infections,  
298 and in ointments for articular pain, burn wounds, and ulcer among other traditional uses.<sup>25,26</sup>

299  
300 Our findings show that *P. lentiscus* L. fruit cyclohexane extract (PLFE1) contains potent  
301 inhibitory compounds that restrict *P. aeruginosa* virulence by abolishing pyocyanin pigment  
302 production, which is known to facilitate colonization of the host and subsequent infection.<sup>6,7</sup>  
303 This anti-virulence activity does not perturb growth and cell viability, which can minimize  
304 selective pressures towards the development of resistance compared to conventional  
305 antibiotics.<sup>28</sup> Nonetheless, additional investigations need to be undertaken to assess whether  
306 *P. aeruginosa* can develop resistance towards PLFE1 upon repeated exposure. Further, by  
307 exploring the mechanistic behind the anti-pyocyanin activity, we have shown that PLFE1  
308 interferes with the HAQs QS-molecules production. Since for *P. aeruginosa* infections QS is

309 the master regulator involved in the expression of many virulence factors such as phenazines,  
310 exoproteases (elastase, alkaline protease), siderophores, and toxins among others, its  
311 inhibition represents a valuable adjuvant therapy that might be used to potentiate the activity  
312 of the available antibiotics applied to handle early *P. aeruginosa* infections.<sup>19,30</sup> In the last five  
313 years there was a large amount of published investigations reporting natural products  
314 highlighting their potential in targeting bacterial virulence factors.<sup>21</sup> Several plant-derived  
315 compounds that belong to alkaloids, organosulfurs, coumarins, flavonoids, phenolic acids,  
316 phenylpropanoids, terpenoids among other chemical classes have been found to be active  
317 against pyocyanin pigment production.<sup>21</sup> However, there is still a significant lack on the specific  
318 underlying molecular mechanisms of action.

319

320 One important finding of the present study was that membrane stiffness in *P. aeruginosa* has  
321 significantly increased upon exposure to PLFE1. Furthermore, we demonstrate that PLFE1  
322 decreases the expression of the ECF $\sigma$  SigX, which is involved in the regulation of membrane  
323 lipid composition,<sup>11,15</sup> and thus, triggers modifications on membrane fluidity and homeostasis.  
324 Accordingly, our data show a decreased expression levels of *accA* and *accB* encoding subunits  
325 of the biotin-dependent enzyme acetyl-CoA carboxylase complex (ACC) that catalyzes the first  
326 step in fatty acid biosynthesis in *P. aeruginosa*.<sup>31</sup> In addition, *fabY* (PA5174) encoding the  $\beta$ -  
327 keto acyl synthase (FabY) involved in fatty acid biosynthesis, is another gene that showed  
328 decreased expression in presence of the PLFE1. Interestingly, these results mirror those  
329 observed in *P. aeruginosa sigX* mutant and over-expressing strains when compared to the  
330 wild-type strain.<sup>11,15,16</sup> Moreover,  $\Delta sigX$  cells display reduced membrane fluidity (membrane  
331 rigidification), HAQs QS-molecules production, pyocyanin pigment production, and virulence  
332 towards a *C. elegans* model.<sup>9,16</sup> Overall, these data provide evidences that PLFE1 most likely  
333 contain membrane-interactive compounds, as it is the case for many plant extracts.<sup>32,33</sup> PLFE1

334 interaction with membrane lipid bilayers seems to be involved in the increased membrane  
335 stiffness, which might trigger the modulation of the ECF $\sigma$  SigX. Thus, our discoveries propose  
336 that PLFE1 exerts its anti-virulence activity through a new potential mechanism that at least  
337 involves the ECF $\sigma$  SigX since no impact of PLFE1 was observed in membrane fluidity of the  
338  $\Delta sigX$  mutant strain.

339

340 Herein, the fractionation of PLFE1 led to the isolation and identification of fractions mainly  
341 enriched in C17:1 and C15:0 ginkgolic acids (GA) or a mix of both GA (C17:1/C15:0). To the  
342 best of our knowledge, the presence of these chemical constituents in *P. lentiscus* L. fruit has  
343 never been previously reported. However, according to the literature, GA has already been  
344 isolated from *Ginkgo biloba* that has long been used in traditional Chinese medicine.<sup>34</sup> The GA  
345 are a mixture of several 2-hydroxy-6-alkylbenzoic acid congeners that differ in carbon alkyl  
346 group length and unsaturation and are structurally similar to salicylic acid, which is reported to  
347 impact negatively the pathogenicity of *P. aeruginosa* PA14 strain by repressing pyocyanin,  
348 elastase, and protease production.<sup>35</sup> A number of pharmacological effects have been attributed  
349 to GA, such as anti-bacterial, anti-fungal, insecticidal, anti-tumour, and neuroprotective effects  
350 among others.<sup>36–39</sup> Moreover, GA are also proven to be effective as anti-biofilm molecules  
351 against bacterial pathogens such as *Escherichia coli* O157:H7 strain, *Staphylococcus aureus*,  
352 *Streptococcus mutans*, *Salmonella spp.*, and *Listeria spp.*<sup>40–42</sup> In line with our results,  
353 antibacterial activity studies show that GA did not affect Gram-negative bacteria survival,  
354 however, they exhibit strong anti-microbial activity against Gram-positive bacteria.<sup>39,40,43,44</sup>  
355 Interestingly, our results indicate that PLFE1 anti-virulence properties can be mostly attributed  
356 to the identified GA-enriched fractions (C17:1, C15:0, C17:1/C15:0) since they are able to  
357 function as pyocyanin production inhibitors without negative effect on bacterial growth.  
358 Moreover, these GA-enriched fractions are capable of inducing *P. aeruginosa* membrane



359 rigidification (*data not shown*). This result is supported by the fact that the lipid soluble  
360 components of the cell wall of Gram-negative bacteria is shown to intercept GA compounds.<sup>43</sup>

361

362 Following demonstration of PLFE1 and GA-enriched fractions for their *in vitro* anti-virulence  
363 properties against *P. aeruginosa*, we assayed them for *in vivo* efficacy using the human lung  
364 A549 cells and the nematode *C. elegans* as models host. In both infection models, the virulence  
365 of *P. aeruginosa* upon exposure to PLFE1 at a dose of 100 µg/mL is shown to be significantly  
366 attenuated. Further, the evaluation of the cytotoxicity of PLFE1 and GA molecules using A549  
367 lung human cells indicated no or slight cytotoxicity at IC<sub>50</sub> values. Taken together, these studies  
368 deliver a promising perspective for the potential future development of PLFE1 or GA molecules  
369 as an adjuvant agent to fight against *P. aeruginosa* infections. Nonetheless, it remains to be  
370 verified whether PLFE1 or GA molecules have an antibiotic-potentiating activity, both *in vitro*  
371 and *in vivo*, against the pathogen *P. aeruginosa*.

372

## 373 **CONCLUSION**

374 Overall, the data of this study suggest that the anti-virulence efficacy of PLFE1 and GA-  
375 enriched fractions might possibly be attributed to their interaction with the lipid bilayer  
376 membranes of *P. aeruginosa* resulting in the modification of membrane fluidity. Therefore, the  
377 increased membrane stiffness in presence of PLFE1 and GA-enriched fractions appears to be  
378 mediated through the modulation of the ECF $\sigma$  SigX, which is known to be involved in the  
379 regulation of *P. aeruginosa* virulence. These findings need further experimental evidences, not  
380 least in terms of identifying the specific molecular mechanisms of action leading to impact the  
381 ECF $\sigma$  SigX as being a potential molecular target to alter the expression of virulence in *P.*  
382 *aeruginosa*.



## 383 **METHODS**

384 **Bacterial strains, media and growth conditions.** The *P. aeruginosa* H103, H103-pAB-PsigX,  
385 and H103- $\Delta$ sigX<sup>27</sup> used in this study are all derivatives of *P. aeruginosa* wild-type PAO1.  
386 Planktonic cultures were grown aerobically at 37 °C in LB broth on a rotary shaker (180 rpm)  
387 from an initial inoculum adjusted to an OD at 580 nm of 0.08. The antibiotics stock solutions  
388 used in this study were sterilized by filtration through 0.22- $\mu$ m filters, aliquoted into daily-use  
389 volumes and kept at -20 °C.

390

391 **Collection and preparation of *P. lentiscus* L. fruit extracts.** Fruits of *P. lentiscus* L. were  
392 collected within the wilaya of Jijel, Algeria, in September 2016, with the collect agreement  
393 (48/MC/DGCE/DSPEC/2016) delivered by the Research Centre on Analytical Chemistry  
394 (CRAPC). A voucher herbarium specimen is deposited in the herbarium of PNAS laboratory,  
395 Université Paris Descartes (France). A sample of 8.98 g of fruits was subjected to a pressurized  
396 solvent extraction (PSE) using a Speed Extractor E-914 (Büchi) equipped with four cells (120  
397 mL) and a collector with four flat bottom vials (220 mL) successively with cyclohexane, ethyl  
398 acetate, methanol, and water. Maximum pressure and temperature were adjusted to 100 bar  
399 and to 50 °C, respectively. Two extraction cycles with a hold-on time of 15 min were performed  
400 in each case. Solvents were removed under reduced pressure. A total of 4 extracts were  
401 obtained (Supplementary Table S3). Solutions at 10 mg mL<sup>-1</sup> were prepared in DMSO of each  
402 extract and stored at 4 °C until use.

403

404 **Pyocyanin quantification assay.** To perform pyocyanin pigment quantification assay, *P.*  
405 *aeruginosa* H103 cells untreated (grown in presence of 1% DMSO) and treated with 100, 50,  
406 25, 12.5, 6.25, 3.12, 1.6 and 0.8  $\mu$ g mL<sup>-1</sup> of *P. lentiscus* L. fruit extracts (PLFE1-4) or ginkgolic

407 acid-enriched fractions (PLFE1-(2-4)) were grown on 96-well microtiter plate for 24 h at 37 °C  
408 on a rotary shaker (180 rpm). Then, supernatants samples were collected by centrifugation  
409 and extracted with chloroform. The chloroform layer (blue layer) was acidified by adding 0.5 M  
410 HCl. The absorbance of the HCl layer (pink layer) was recorded at 520nm using the Spark 20M  
411 multimode Microplate Reader controlled by SparkControl™ software Version 2.1 (Tecan Group  
412 Ltd.) and the data were normalized for bacterial cell density (OD<sub>580nm</sub>).

413

414 **Virulence attenuation of *P. aeruginosa* using human lung A549 line cells.**The human lung  
415 A549 cells were cultured in Dulbecco's Modified Eagle's Medium (DMEM, Lonza,  
416 BioWhittaker®) supplemented with 4.5 g L<sup>-1</sup> glucose, L-Glutamine, 10% heat-inactivated (30  
417 min, 56 °C) fetal bovine serum (FBS), and 100 Units mL<sup>-1</sup> each of penicillin and streptomycin  
418 antibiotics. Cells were grown at 37 °C under the atmosphere of 5% CO<sub>2</sub> and 95% air with  
419 regularly medium change until a confluent monolayer was obtained. The anti-virulence effect  
420 of PLFE1 or ginkgolic acid-enriched fractions (PLFE1-(2-4)) on *P. aeruginosa* H103 was  
421 determined using an enzymatic assay (Pierce™ LDH Cytotoxicity Assay Kit, Thermo  
422 Scientific™), which measures lactate dehydrogenase (LDH) released from the cytosol of  
423 damaged A549 cells into the supernatant. After overnight incubation with *P. aeruginosa* H103  
424 (10<sup>8</sup> CFU mL<sup>-1</sup>) previously treated or untreated (control condition), the supernatants from  
425 confluent A549 monolayers grown on 24-well tissue culture plates were collected and the  
426 concentration of the LDH release was quantified. A549 cells exposed to 1X Lysis Buffer were  
427 used as a positive control of maximal LDH release (100% lysis) as specified by the  
428 manufacturer's recommendations. The background level (0% LDH release) was determined  
429 with serum free culture medium. The LDH release assays were also used to determine the  
430 cytotoxicity of PLFE1 or ginkgolic acid-enriched fractions (PLFE1-(2-4)) in A549 cells upon  
431 direct exposure after 1-, 3-, 6-, and 24-h incubation.

432

433 ***Caenorhabditis elegans* fast-killing infection assay.** The *C. elegans* wild-type Bristol strain  
434 N2 worms were grown at 22 °C on nematode growth medium (NGM) agar plates using  
435 *Escherichia coli* OP50 as a food source. The *P. aeruginosa*-*C. elegans* fast-kill infection assay  
436 was performed as described previously<sup>45</sup> with minor modifications. Briefly, cultures of *P.*  
437 *aeruginosa* H103 strain untreated or treated with PLFE1 at 100 µg mL<sup>-1</sup> were seeded on a 24-  
438 well plate containing in each well 1 mL of Peptone-Glucose-Sorbitol (PGS) agar. Control wells  
439 were seeded with 25 µL of *E. coli* OP50 from an overnight culture. The plate was then incubated  
440 at 37 °C for 24 h to make bacterial lawns and then shifted to 22 °C for 4 h. For each assay, 15  
441 to 20 L4-synchronized worms were added to the killing and control lawns and incubated at 22  
442 °C. Worm survival was scored at 4-, 6-, 8-, 20-, and 24-h after the start of the assay, using an  
443 Axiovert S100 optical microscope (Zeiss).

444

445 **Bacterial cell viability assays by flow cytometry.** Cell viability assays of *P. aeruginosa* H103  
446 cells untreated and treated by different concentrations of *P. lentiscus* L. fruit extract (PLFE1)  
447 were assessed by using the LIVE/DEAD™ BacLight™ Bacterial Viability and Counting Kit, for  
448 flow cytometry (Invitrogen, Molecular Probes). Briefly, *P. aeruginosa* H103 untreated and  
449 treated suspensions were diluted in filter-sterilized PBS to reach a final density of 1 x 10<sup>6</sup> CFU  
450 mL<sup>-1</sup>, then stained following the manufacturer's instructions. The data were acquired using  
451 CytoFlex S flow cytometer (Beckman coulter Life science). An aliquot of cells was killed with  
452 100% ethanol and used as a control of death cells. The SYTO9 stained cells were detected by  
453 an excitation with 22 mW blue laser at 488 and with emission wavelength at 525 nm (green,  
454 with band pass filter of 40 nm), while the PI (Propidium iodide) stained cells were detected by  
455 690 nm (red, with band pass filter of 50 nm).

456

457 **Extraction and quantification of HAQs.** Planktonic cultures of *P. aeruginosa* H103 untreated  
458 (control DMSO 1%) and treated by 100, 50, 25, 12.5, 6.25, 3.12, 1.6 and 0.8  $\mu\text{g mL}^{-1}$  of PLFE1  
459 were subjected to HAQ molecules extraction following the technique described in a previous  
460 study.<sup>46</sup> HAQs were quantified by a combined spectrophotometer/luminometer microplate  
461 assay using the biosensor strain PAO1 *pqsA* CTX-*lux::pqsA*.<sup>47</sup> The HAQ biosensor strain was  
462 grown overnight and OD was measured and adjusted with fresh LB medium to achieve OD<sub>580nm</sub>  
463 of 1. For each test well, 5  $\mu\text{L}$  of HAQs crude extracts were diluted in 100  $\mu\text{L}$  of LB and added  
464 to 100  $\mu\text{L}$  of 1 in 50 dilution of the HAQ biosensor strain. Further, bioluminescence and OD<sub>580nm</sub>  
465 were monitored in specialized white sided and clear bottom 96-well microtiter plate every 15  
466 min for 24 h at 37 °C using the Spark 20M multimode Microplate Reader controlled by  
467 SparkControl™ software Version 2.1 (Tecan Group Ltd.). Both HHQ and PQS synthetic  
468 standards (Sigma-Aldrich) at a final concentration of 5  $\mu\text{M}$ , used as positive controls, were  
469 added to 1 in 100 dilution of the HAQ biosensor strain, as both activate bioluminescence  
470 production. The recorded bioluminescence as relative light units (R.L.U) were normalized to  
471 OD<sub>580nm</sub> of cultures suspensions.

472

473 **Membrane fluidity measurement by fluorescence anisotropy.** Fluorescence anisotropy  
474 analysis of *P. aeruginosa* cells were performed as previously described.<sup>16</sup> Briefly, cell pellets  
475 of *P. aeruginosa* H103 untreated (control DMSO 1%) and treated by 100, 50, 25, 12.5, 6.25,  
476 3.12, 1.6 and 0.8  $\mu\text{g mL}^{-1}$  of PLFE1 were washed two times ( $7500 \times g$ , 5 min, 25 °C) in 0.01 M  
477  $\text{MgSO}_4$  and resuspended in the same wash solution to reach an OD<sub>580nm</sub> of 0.1. One  $\mu\text{L}$  of a 4  
478 mM of 1,6-diphenyl-1,3,5-hexatriene (DPH) stock solution (Sigma-Aldrich) in tetrahydrofuran  
479 was added to 1 mL aliquot of the resuspended cultures and incubated in the dark for 30 min at  
480 37 °C to allow the probe to incorporate into the cytoplasmic membrane. Measurement of the  
481 fluorescence polarization was performed using the Spark 20M multimode Microplate Reader,

482 equipped with an active temperature regulation system (Te-Cool™, Tecan Group Ltd.).  
483 Excitation and emission wavelengths were set to 365 nm and 425 nm, respectively, and the  
484 Fluorescence Anisotropy (FA) was calculated according to Lakowicz.<sup>48</sup> Three measurements  
485 were performed for each sample and data were recorded using SparkControl™ software  
486 (Version 2.1, Tecan Group Ltd.). The relationship between fluorescence polarization and  
487 membrane fluidity is an inverse one, where increasing anisotropy values correspond to a more  
488 rigid membrane and vice versa. All values are reported as means of triplicate analyses for each  
489 experimental variable.

490

491 **Transcriptional fusion *PsigX::luxCDABE* construction and *sigX* promoter activity**  
492 **analysis in response to PLFE1.** The promoter region of the *sigX* gene (*PsigX*) was amplified  
493 by PCR with primers *PsigX-SacI*-F and *PsigX-SpeI*-R (Supplementary Table S4,) incorporating  
494 *SacI* and *SpeI* linkers, respectively. The promoter region of *sigX* gene was fused to the  
495 *luxCDABE* cassette in the promoterless pAB133 vector.<sup>49</sup> Upon amplification, DNA was  
496 digested with the appropriate restriction enzymes, and cloned into pAB133 generating pAB-  
497 *PsigX* vector. The pAB-*PsigX* plasmid was then transformed separately into one shot™ *E. coli*  
498 TOP10 competent cells (Invitrogen). The constructions were confirmed by DNA sequencing  
499 (Sanger sequencing services, Genewiz). Finally, the plasmids were transferred by  
500 electroporation into *P. aeruginosa* H103 strain. Promoter activity was analysed by monitoring  
501 bioluminescence during course time.

502

503 **Reverse transcription-quantitative PCR analyses (RT-qPCR).** Total RNAs from three  
504 independent H103 untreated and treated cultures with PLFE1 at 100, 25, and 6.25 µg mL<sup>-1</sup>  
505 were isolated by the hot acid-phenol method<sup>27</sup> followed by treatment with Turbo DNA-free™ kit  
506 (Invitrogen) according to the manufacturer's protocol. Synthesis of cDNAs and RT-qPCR were

507 achieved as previously described<sup>50</sup> using the oligonucleotides listed in Supplementary Table  
508 S4. The mRNAs levels were calculated by comparing the threshold cycles (Ct) of target genes  
509 with those of control sample groups and the relative quantification was measured using the  
510  $2^{-\Delta\Delta C_t}$  method<sup>51</sup> using DataAssist<sup>TM</sup> software (Applied Biosystems).

511

512 **PLFE1 fractionation.** Two hundred mg of PLFE1 were subjected to fractionation by medium  
513 MPLC on 9.6 g of silice 60 M with cyclohexane/ethyl acetate as mobile phase solvent mixture  
514 with increasing polarity. A total of 13 fractions were recovered and designated PLFE1-(1-13)  
515 (Supplementary Table S2)

516

517 **Structure determination of compounds present in PLFE1-(2-4) fractions by NMR and**

518 **ozonolysis.** To determine the structure of the main compounds of PLFE1-(2-4), <sup>1</sup>D and <sup>2</sup>D

519 NMR experiments were conducted in a Bruker 400 MHz spectrometer apparatus and recorded

520 in deuterated chloroform (CDCl<sub>3</sub>). To identify the double bond position of the main compound

521 identified in PLFE1-2, an ozonolysis reaction was carried out. Briefly, a solution of 10 mg (0.027

522 mmol, 1.0 equiv) of PLFE1-2 was put in a round bottom flask containing 20 mL of distilled

523 dichloromethane and a small amount of Sudan III. A stream of ozone (O<sub>3</sub>) was bubbled into

524 the solution at -78 °C until the pink solution became colorless (10 min). Then, 200 µL of

525 dimethyl sulphide ((CH<sub>3</sub>)<sub>2</sub>S) (2.7 mmol, 100 equiv) were added to the reaction mixture and

526 stirred for 1 h at 20 °C. From the reaction mixture, 1 µl was directly analyzed by GC-MS.

527

528 **Gas chromatography-mass spectrometry (GC-MS) analyses.** The GC-MS analyses were

529 carried out in a Hewlett Packard GC 6890/MSD 5972 apparatus equipped with HP-5 (30 m x

530 0.25 mm x 0.25 µm). Carried gas was Ar with a flow of 0.9 mL min<sup>-1</sup>, split 1:20, oven was

531 programmed increasing from 180°C to 270°C at 8°C min<sup>-1</sup> with an initial and final hold of 1 and

532 65 min, respectively. The inlet and GC-MS interface temperature were kept at 240 °C. The  
533 temperature of EI (electron impact) 70 eV was 220°C with full scan (80-500 m/z). The injection  
534 volume was 1 µL. Identification of constituents was achieved by comparing their mass spectra  
535 with those of the Mass Spectra Library (NIST 98) compounds.

536

537 **Statistical analyses.** Statistical significance was evaluated using R ([https://www.r-](https://www.r-project.org)  
538 [project.org](https://www.r-project.org)).<sup>52</sup> The data were statistically analyzed using two-sample unpaired two-tailed *t* test  
539 to calculate *P* values. The mean with standard error of the mean (SEM) of at least three  
540 independent biological experiments were calculated and plotted. *C. elegans* survival curves  
541 were prepared using R to perform a statistical log-rank (Mantel-Cox) test.

542

## 543 **DATA AVAILABILITY**

544 The authors declare that all relevant data supporting the findings of the study are available in  
545 this article and its Supplementary Information files, or from the corresponding author upon  
546 request.

547

## 548 **ACKNOWLEDGMENTS**

549 The LMSM is supported by the Région Normandie (France), Evreux Portes de Normandie  
550 (France) and European FEDER funds. PNAS and CRAPC are partners of the European  
551 Union's H2020-MSCA-RISE-2015 EXANDAS (Exploitation of aromatic plants' by-products for  
552 the development of novel cosmeceuticals and food supplements, Grant Agreement 691247).

553 A.T. is supported by a post-doctoral fellowship from European Union (FEDER) and Région  
554 Normandie (France). D.T. is supported by a doctoral fellowship from the Région Normandie  
555 (France). C. A. was the recipient of a postgraduate fellowship from Campus France and FUNAI  
556 (Nigeria). S.O is supported by a CONICYT's scholarship (Comisión Nacional de Investigación  
557 Científica y Tecnológica from Chile). The funders had no role in study design, data collection  
558 and interpretation, or the decision to submit this work for publication. We gratefully  
559 acknowledge Prof. Paul Williams (Centre for Biomolecular Sciences, University of Nottingham)  
560 for providing PAO1  $\Delta pqsA$  CTX-  $pqsA::lux$  biosensor strain and Mr. Abdelhamid Boudjerda for  
561 plant material collection.

562

## 563 **COMPETING INTERESTS**

564 The authors declare no competing interests.

565



566 **AUTHOR CONTRIBUTIONS**

567 A.T., S.C., E.B., S.B., R.G., and O.L. conceived and designed the experiments; A.T., S.O.,  
568 O.C.A., N.B., O.M., and D.T. conducted experiments and analyzed the data; A.T., S.C., P.C.,  
569 E.B., S.O., M.K., S.C., S.M., M.F., and N.O. contributed to the writing of the manuscript. All  
570 authors proofread the final draft and approved the final manuscript.

571

## 572 **FIGURE LEGENDS**

573 **Figure 1.** *P. lentiscus* L. fruit extract (PLFE) is a potent inhibitor of pyocyanin production in *P.*  
574 *aeruginosa* strain H103. **(A)** Effect of various concentrations of *P. lentiscus* cyclohexane  
575 (PLFE1), ethyl acetate (PLFE2), methanol (PLFE3), and water (PLFE4) extracts on pyocyanin  
576 production. **(B)** Relative expression levels of representative genes from phenazine  
577 biosynthesis pathway in H103 treated with PLFE1 at 100, 25, and 6.25  $\mu\text{g mL}^{-1}$  compared to  
578 the relative mRNA levels in the control condition (H103 untreated). Values represent the mean  
579 ( $\pm$  SEM) of three independent assays. Statistics were achieved by a two-tailed *t* test: \*\*\*\*,  
580  $P < 0.0001$ ; \*\*\*,  $P = 0.0001$  to  $0.001$ ; \*\*,  $P = 0.001$  to  $0.01$ ; \*,  $P = 0.01$  to  $0.05$ ; NS (Not Significant),  $P \geq 0.05$ .

581

582 **Figure 2.** Virulence attenuation on *P. aeruginosa* by PLFE1. **(A)** Anti-virulence effects of  
583 PLFE1 in human A549 lung cells infection model. The presence of PLFE1 ( $100 \mu\text{g mL}^{-1}$ )  
584 significantly protected A549 lung cells from lysis after 20h infection. Data are presented as the  
585 mean  $\pm$  SEM values of four independent experiments performed in duplicate. \*\*  $P = 0.001$  to  
586  $0.01$  (two-tailed *t* test) versus untreated cells. **(B)** *P. aeruginosa* H103 virulence attenuation in  
587 a *C. elegans* infection model by PLFE1. Sixty L4-stage nematodes per experimental group  
588 were placed on lawns of *E. coli* OP50 (black) or H103 strain in the absence (red) or presence  
589 of PLFE1 at  $100 \mu\text{g mL}^{-1}$  (green). Alive nematodes were scored at 4-, 6-, 8-, 20- and 24-h after  
590 the start of the assay. \*\*\*\*,  $P < 0.0001$  (log-rank [Mantel-Cox] test) versus untreated cells.

591

592 **Figure 3.** PLFE1 decreases HAQ-molecules production. **(A)** Normalized mean maximal  
593 bioluminescence output from the HAQ-biosensor strain in the presence of crude ethyl acetate  
594 HAQs extracts prepared from cultures of H103 treated with different concentrations of PLFE1  
595 compared to positive control conditions (HHQ and PQS at  $5 \mu\text{M}$ ; HAQs crude ethyl acetate  
596 extract from H103 untreated) and to negative control conditions (HAQs crude ethyl acetate  
597 extract from HAQ-biosensor strain and LB medium). **(B)** Relative expression levels of  
598 representative genes from HAQ QS system in H103 treated with PLFE1 at 100, 25, and 6.25  
599  $\mu\text{g mL}^{-1}$  compared to the relative mRNA levels in the control condition (H103 untreated). Values  
600 represent the mean ( $\pm$  SEM) of three independent assays. Statistics were achieved by a two-  
601 tailed *t* test: \*\*\*,  $P = 0.0001$  to  $0.001$ ; \*\*,  $P = 0.001$  to  $0.01$ ; \*,  $P = 0.01$  to  $0.05$ ; NS (Not Significant),  
602  $P \geq 0.05$ .

603

604 **Figure 4.** PLFE1 induces membrane stiffness. **(A)** Fluorescence anisotropy (membrane  
605 fluidity) measurements in *P. aeruginosa* strain H103 exposed to various concentrations of  
606 PLFE1 compared to the control condition (H103 untreated). **(B)** Relative expression levels of  
607 *sigX* encoding the SigX extracytoplasmic function sigma factor (ECF $\sigma$ ) and its known target  
608 genes (*accA*, *accB*, and *fabY*) involved in fatty acid biosynthesis in H103 treated with PLFE1  
609 at 100, 25, and 6.25  $\mu\text{g mL}^{-1}$  compared to the relative mRNA levels in the control condition  
610 (H103 untreated). **(C)** Relative bioluminescence levels of H103 harboring the pAB-*PsigX*  
611 plasmid (*sigX* promoter region) treated with PLFE1 at 100, 25, and 6.25  $\mu\text{g mL}^{-1}$  compared to  
612 the relative bioluminescence levels in the control condition (H103-pAB-*PsigX* untreated). Data  
613 at both transition and stationary phases are displayed. Values represent the mean ( $\pm$  SEM) of  
614 three independent assays. Statistics were achieved by a two-tailed *t* test: \*\*\*\*,  $P < 0.0001$ ; \*\*\*,  
615  $P = 0.0001$  to  $0.001$ ; \*\*,  $P = 0.001$  to  $0.01$ ; \*,  $P = 0.01$  to  $0.05$ ; NS (Not Significant),  $P \geq 0.05$ .

616  
617 **Figure 5.** Chemical structures of ginkgolic acid derivatives identified in PLFE1-(2-4).

618  
619 **Figure 6.** Effect of GA-enriched fractions from PLFE1 on *P. aeruginosa* virulence. **(A)**  
620 Pyocyanin production upon exposure to different concentrations of GA-enriched fractions. **(B)**  
621 Anti-virulence of GA-enriched in human A549 lung cells infection model. The presence of GA-  
622 enriched fractions ( $100 \mu\text{g mL}^{-1}$ ) significantly protected A549 lung cells from lysis after 20 h  
623 infection. Data are presented as the mean  $\pm$  SEM values of four independent experiments  
624 performed in duplicate. Statistics were achieved by a two-tailed *t* test: \*\*,  $P = 0.001$  to  $0.01$ ; \*,  
625  $P = 0.01$  to  $0.05$ .

626  
627 **Figure 7.** Cytotoxic effect of PLFE1 and its GA-enriched fractions on human lung A549 line  
628 cells. **(A)** PLFE1 was assayed at different concentrations. **(B)** Cytotoxicity of GA-enriched  
629 fractions exhibiting pyocyanin production inhibition. LDH release was determined at 1 h, 3 h, 6  
630 h, and 24 h. DMSO was used as a vehicle control. Data are displayed as the mean  $\pm$  SEM  
631 values of four independent experiments performed in duplicate. Statistics were achieved by a  
632 two-tailed *t* test: \*\*\*,  $P = 0.0001$  to  $0.001$ ; \*\*,  $P = 0.001$  to  $0.01$ ; \*,  $P = 0.01$  to  $0.05$ ; NS (Not Significant),  
633  $P \geq 0.05$ .

634  
635

## 636 REFERENCES

- 637 1. Pendleton, J. N., Gorman, S. P. & Gilmore, B. F. Clinical relevance of the ESKAPE  
638 pathogens. *Expert Rev Anti Infect Ther* **11**, 297–308 (2013).  
639
- 640 2. Global priority list of antibiotic-resistant bacteria to guide research, discovery, and  
641 development of new antibiotics. *World Health Organization* (2017).  
642
- 643 3. Malhotra, S., Hayes, D. & Wozniak, D. J. Cystic fibrosis and *Pseudomonas aeruginosa*:  
644 the host-microbe interface. *Clin Microbiol Rev* **32**, e00138-18 (2019).  
645
- 646 4. Moradali, M. F., Ghods, S. & Rehm, B. H. A. *Pseudomonas aeruginosa* lifestyle: A  
647 paradigm for adaptation, survival, and persistence. *Front Cell Infect Microbiol* **7**, 39 (2017).  
648
- 649 5. Price-Whelan, A., Dietrich, L. E. P. & Newman, D. K. Rethinking “secondary”  
650 metabolism: Physiological roles for phenazine antibiotics. *Nat Chem Biol* **2**, 71–78 (2006).  
651
- 652 6. Lau, G. W., Hassett, D. J., Ran, H. & Kong, F. The role of pyocyanin in *Pseudomonas*  
653 *aeruginosa* infection. *Trends Mol Med* **10**, 599–606 (2004).  
654
- 655 7. Hall, S. *et al.* Cellular effects of pyocyanin, a secreted virulence factor of *Pseudomonas*  
656 *aeruginosa*. *Toxins* **8**, 236 (2016).  
657
- 658 8. Mavrodi, D. V. *et al.* Functional analysis of genes for biosynthesis of pyocyanin and  
659 phenazine-1-carboxamide from *Pseudomonas aeruginosa* PAO1. *J Bacteriol* **183**, 6454–6465  
660 (2001).  
661
- 662 9. Gicquel, G. *et al.* The extra-cytoplasmic function sigma factor *sigX* modulates biofilm  
663 and virulence-related properties in *Pseudomonas aeruginosa*. *PLoS One* **8**, e80407 (2013).  
664
- 665 10. Chevalier, S. *et al.* Extracytoplasmic function sigma factors in *Pseudomonas*  
666 *aeruginosa*. *Biochim Biophys Acta - Gene Regul Mech* **1862**, 706–721 (2019).  
667
- 668 11. Blanka, A. *et al.* Identification of the alternative sigma factor SigX regulon and its  
669 implications for *Pseudomonas aeruginosa* pathogenicity. *J Bacteriol* **196**, 345–356 (2014).  
670
- 671 12. Otero-Asman, J. R., Wettstadt, S., Bernal, P. & Llamas, M. A. Diversity of  
672 extracytoplasmic function sigma ( $\sigma^{\text{ECF}}$ ) factor-dependent signaling in *Pseudomonas*. *Mol*  
673 *Microbiol* **112**, 356–373 (2019).  
674
- 675 13. Schulz, S. *et al.* Elucidation of sigma factor-associated networks in *Pseudomonas*  
676 *aeruginosa* reveals a modular architecture with limited and function-specific crosstalk. *PLOS*  
677 *Pathog* **11**, e1004744 (2015).

- 678  
679 14. Duchesne, R. *et al.* A proteomic approach of SigX function in *Pseudomonas aeruginosa*  
680 outer membrane composition. *J Proteomics* **94**, 451–459 (2013).  
681
- 682 15. Boechat, A. L., Kaihami, G. H., Politi, M. J., Lépine, F. & Baldini, R. L. A novel role for  
683 an ECF sigma factor in fatty acid biosynthesis and membrane fluidity in *Pseudomonas*  
684 *aeruginosa*. *PLoS One* **8**, e84775 (2013).  
685
- 686 16. Fléchard, M. *et al.* The absence of SigX results in impaired carbon metabolism and  
687 membrane fluidity in *Pseudomonas aeruginosa*. *Sci Rep* **8**, 17212 (2018).  
688
- 689 17. Brinkman, F. S. L., Schoofs, G., Hancock, R. E. W. & De Mot, R. Influence of a putative  
690 ECF sigma factor on expression of the major outer membrane protein, OprF, in *Pseudomonas*  
691 *aeruginosa* and *Pseudomonas fluorescens*. *J Bacteriol* **181**, 4746–4756 (1999).  
692
- 693 18. Wagner, S. *et al.* Novel strategies for the treatment of *Pseudomonas aeruginosa*  
694 infections. *J Med Chem* **59**, 5929–5969 (2016).  
695
- 696 19. Soukarieh, F., Williams, P., Stocks, M. J. & Cámara, M. *Pseudomonas aeruginosa*  
697 quorum sensing systems as drug discovery targets: Current position and future perspectives.  
698 *J Med Chem* **61**, 10385–10402 (2018).  
699
- 700 20. Mahady, G. Medicinal plants for the prevention and treatment of bacterial infections.  
701 *Curr Pharm Des* **11**, 2405–2427 (2005).  
702
- 703 21. Silva, L. N., Zimmer, K. R., Macedo, A. J. & Trentin, D. S. Plant natural products  
704 targeting bacterial virulence factors. *Chem Rev* **116**, 9162–9236 (2016).  
705
- 706 22. Calvert, M. B., Jumde, V. R. & Titz, A. Pathoblockers or antivirulence drugs as a new  
707 option for the treatment of bacterial infections. *Beilstein J Org Chem* **14**, 2607–2617 (2018).  
708
- 709 23. AL-Saghir G., M. & Porter M., D. Taxonomic revision of the genus *Pistacia* L.  
710 (*Anacardiaceae*). *Am J Plant Sci* **3**, 12–32 (2012).  
711
- 712 24. Zohary, M. A monographical study of the genus *Pistacia*. *Palest J Bot Jerusalem* **5**, 187–  
713 228 (1952).  
714
- 715 25. Rauf, A. *et al.* Phytochemical, ethnomedicinal uses and pharmacological profile of genus  
716 *Pistacia*. *Biomed Pharmacother* **86**, 393–404 (2017).  
717
- 718 26. Bozorgi, M. *et al.* Five *Pistacia* species (*P. vera*, *P. atlantica*, *P. terebinthus*, *P. khinjuk*,  
719 and *P. lentiscus*): a review of their traditional uses, phytochemistry, and pharmacology.  
720 *ScientificWorldJournal* **2013**, 219815 (2013).  
721

- 722 27. Bouffartigues, E. *et al.* Transcription of the *oprF* gene of *Pseudomonas aeruginosa* is  
723 dependent mainly on the *sigX* sigma factor and is sucrose induced. *J Bacteriol* **194**, 4301–  
724 4311 (2012).  
725
- 726 28. Rasko, D. A. & Sperandio, V. Anti-virulence strategies to combat bacteria-mediated  
727 disease. *Nat Rev Drug Discov* **9**, 117–128 (2010).  
728
- 729 29. Dickey, S. W., Cheung, G. Y. C. & Otto, M. Different drugs for bad bugs: Antivirulence  
730 strategies in the age of antibiotic resistance. *Nat Rev Drug Discov* **16**, 457–471 (2017).  
731
- 732 30. Martínez, O. F., Cardoso, M. H., Ribeiro, S. M. & Franco, O. L. Recent advances in anti-  
733 virulence therapeutic strategies with a focus on dismantling bacterial membrane microdomains,  
734 toxin neutralization, quorum-sensing interference and biofilm inhibition. *Front Cell Infect*  
735 *Microbiol* **9**, 74 (2019).  
736
- 737 31. Kondakova, T. *et al.* Glycerophospholipid synthesis and functions in *Pseudomonas*.  
738 *Chem Phys Lipids* **190**, 27–42 (2015).  
739
- 740 32. Kopeč, W., Telenius, J. & Khandelia, H. Molecular dynamics simulations of the  
741 interactions of medicinal plant extracts and drugs with lipid bilayer membranes. *FEBS J* **280**,  
742 2785–2805 (2013).  
743
- 744 33. Tsuchiya, H. Membrane interactions of phytochemicals as their molecular mechanism  
745 applicable to the discovery of drug leads from plants. *Molecules* **20**, 18923–18966 (2015).  
746
- 747 34. Mahadevan, S. & Park, Y. Multifaceted therapeutic benefits of *Ginkgo biloba* L.:  
748 Chemistry, efficacy, safety, and uses. *J Food Sci* **73**, R14–R19 (2008).  
749
- 750 35. Prithiviraj, B. *et al.* Down regulation of virulence factors of *Pseudomonas aeruginosa* by  
751 salicylic acid attenuates its virulence on *Arabidopsis thaliana* and *Caenorhabditis elegans*.  
752 *Infect Immun* **73**, 5319–5328 (2005).  
753
- 754 36. van Beek, T. A. & Montoro, P. Chemical analysis and quality control of *Ginkgo biloba*  
755 leaves, extracts, and phytopharmaceuticals. *J Chromatogr A* **1216**, 2002–2032 (2009).  
756
- 757 37. Ahlemeyer, B. & Krieglstein, J. Neuroprotective effects of *Ginkgo biloba* extract. *Cell Mol*  
758 *Life Sci* **60**, 1779–1792 (2003).  
759
- 760 38. Satyan, K. S., Jaiswal, A. K., Ghosal, S. & Bhattacharya, S. K. Anxiolytic activity of  
761 ginkgolic acid conjugates from Indian *Ginkgo biloba*. *Psychopharmacology (Berl)* **136**, 148–  
762 152 (1998).  
763
- 764 39. Yang, X., Zhu, W., Chen, J., Qian, Z. & Xie, J. Study on anti-bacterium activity of  
765 ginkgolic acids and their momomers. *Zhong Yao Cai* **27**, 661–663 (2004).

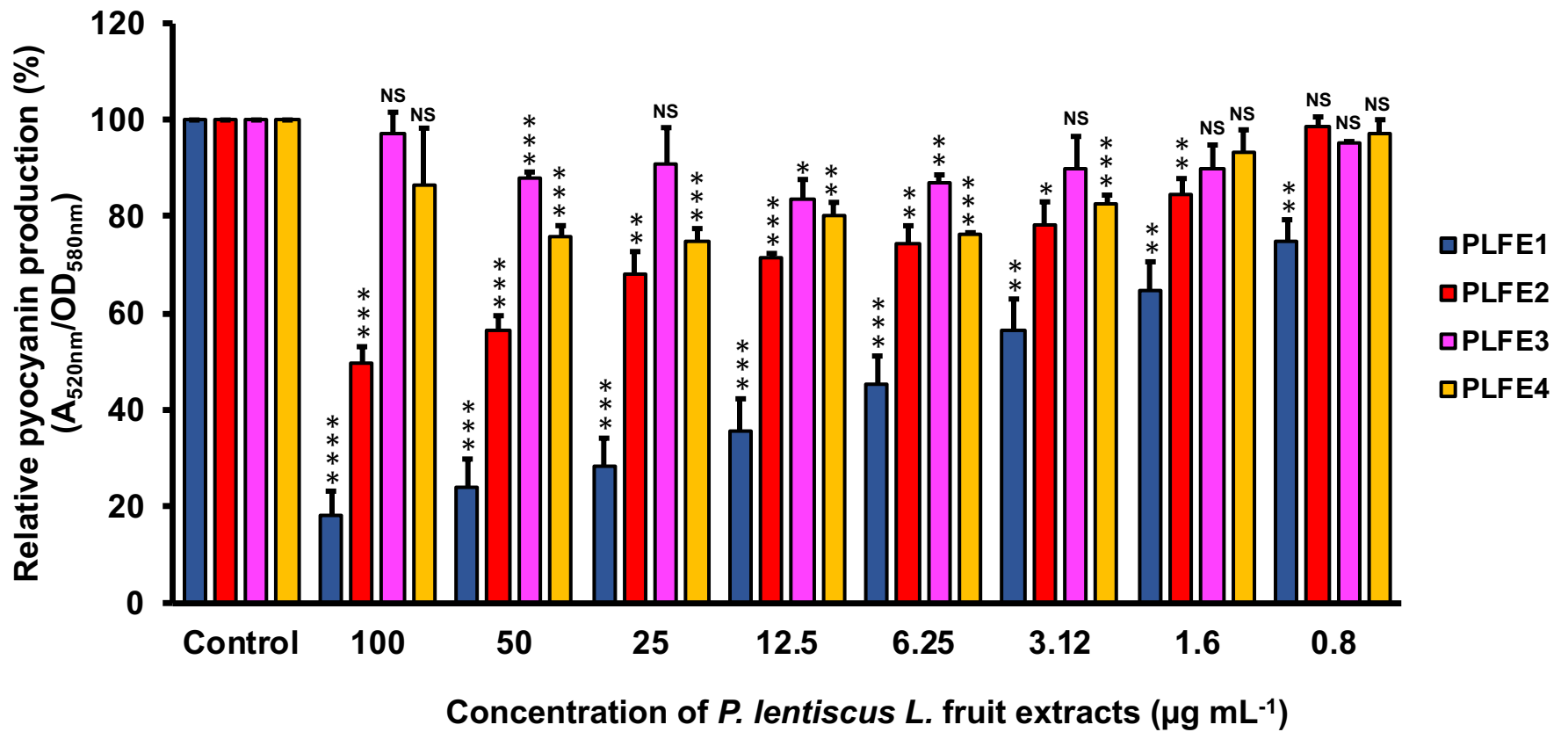


- 766  
767 40. He, J. *et al.* Effects of ginkgoneolic acid on the growth, acidogenicity, adherence, and  
768 biofilm of *Streptococcus mutans in vitro*. *Folia Microbiol (Praha)*. **58**, 147–153 (2013).  
769
- 770 41. Lee, J. H., Kim, Y. G., Ryu, S. Y., Cho, M. H. & Lee, J. Ginkgolic acids and *Ginkgo biloba*  
771 extract inhibit *Escherichia coli* O157: H7 and *Staphylococcus aureus* biofilm formation. *Int J*  
772 *Food Microbiol* **174**, 47–55 (2014).  
773
- 774 42. Wu, Y., Park, K. C., Choi, B. G., Park, J. H. & Yoon, K. S. The antibiofilm effect of *Ginkgo*  
775 *biloba* extract against *Salmonella* and *Listeria* isolates from poultry. *Foodborne Pathog Dis* **13**,  
776 229–238 (2016).  
777
- 778 43. Hua, Z., Wu, C., Fan, G., Tang, Z. & Cao, F. The antibacterial activity and mechanism  
779 of ginkgolic acid C15:1. *BMC Biotechnol* **17**, 5 (2017).  
780
- 781 44. Choi, J. G. *et al.* Antibacterial activity of hydroxyalkenyl salicylic acids from sarcotesta  
782 of *Ginkgo biloba* against vancomycin-resistant *Enterococcus*. *Fitoterapia* **80**, 18–20 (2009).  
783
- 784 45. Blier, A. S. *et al.* C-type natriuretic peptide modulates quorum sensing molecule and  
785 toxin production in *Pseudomonas aeruginosa*. *Microbiology* **157**, 1929–1944 (2011).  
786
- 787 46. Tahrioui, A. *et al.* Extracellular DNA release, quorum sensing, and PrrF1/F2 small RNAs  
788 are key players in *Pseudomonas aeruginosa* tobramycin-enhanced biofilm formation. *npj*  
789 *Biofilms Microbiomes* **5**, 15 (2019).  
790
- 791 47. Fletcher, M. P., Diggle, S. P., Cámara, M. & Williams, P. Biosensor-based assays for  
792 PQS, HHQ and related 2-alkyl-4-quinolone quorum sensing signal molecules. *Nat Protoc* **2**,  
793 1254–1262 (2007).  
794
- 795 48. Lakowicz, J. R. Fluorescence anisotropy in *Principles of Fluorescence Spectroscopy*  
796 (ed. Lakowicz, J. R.) 353–382 (Springer, 2006).  
797
- 798 49. Bazire, A. *et al.* The sigma factor AlgU plays a key role in formation of robust biofilms by  
799 nonmucoid *Pseudomonas aeruginosa*. *J Bacteriol* **192**, 3001–3010 (2010).  
800
- 801 50. Bouffartigues, E. *et al.* The absence of the *Pseudomonas aeruginosa* OprF protein leads  
802 to increased biofilm formation through variation in c-di-GMP level. *Front Microbiol* **6**, 630  
803 (2015).  
804
- 805 51. Pfaffl, M. W. A new mathematical model for relative quantification in real-time RT-PCR.  
806 *Nucleic Acids Res* **29**, 45e–45 (2001).  
807
- 808 52. R Development Core Team. R: A Language and Environment for Statistical Computing  
809 (2017).

# Figure 1

bioRxiv preprint doi: <https://doi.org/10.1101/2020.03.17.995043>; this version posted March 19, 2020. The copyright holder for this preprint (which was not certified by peer review) is the author/funder. All rights reserved. No reuse allowed without permission.

## A



## B

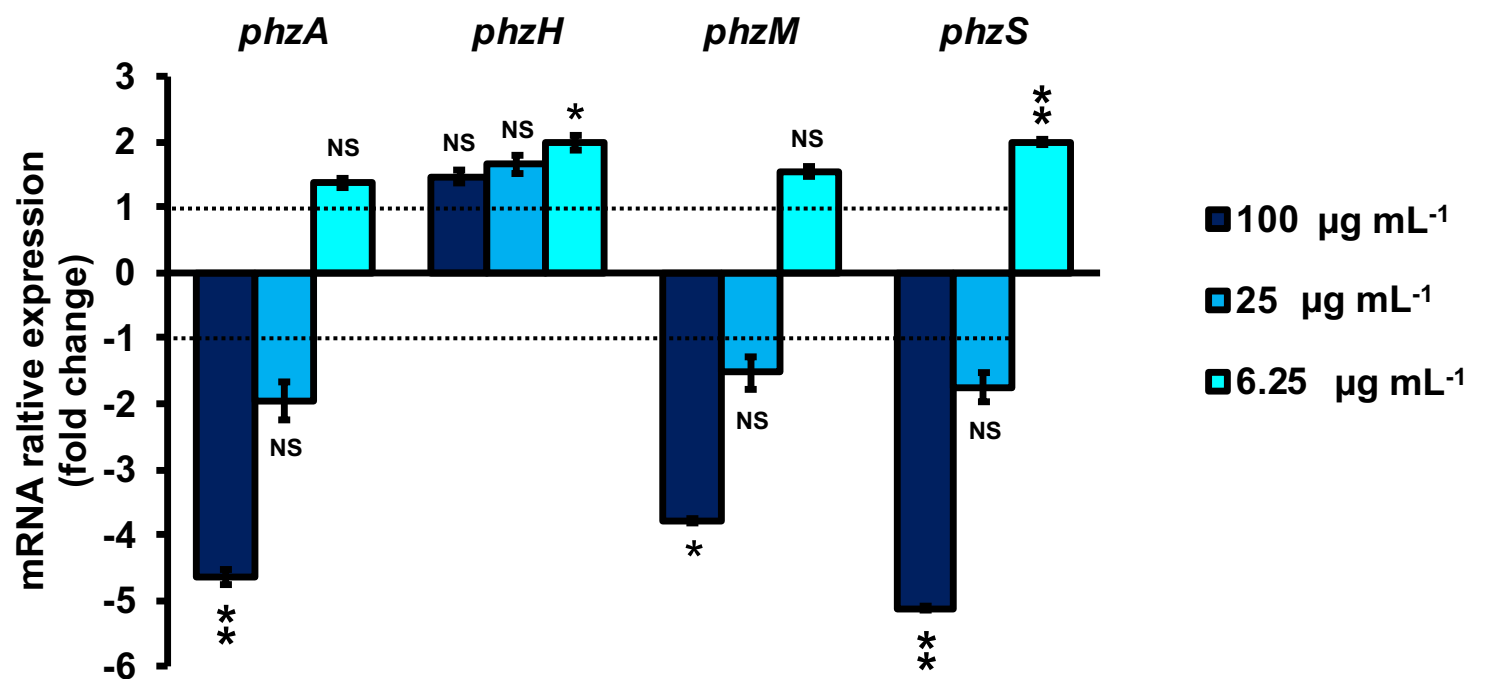
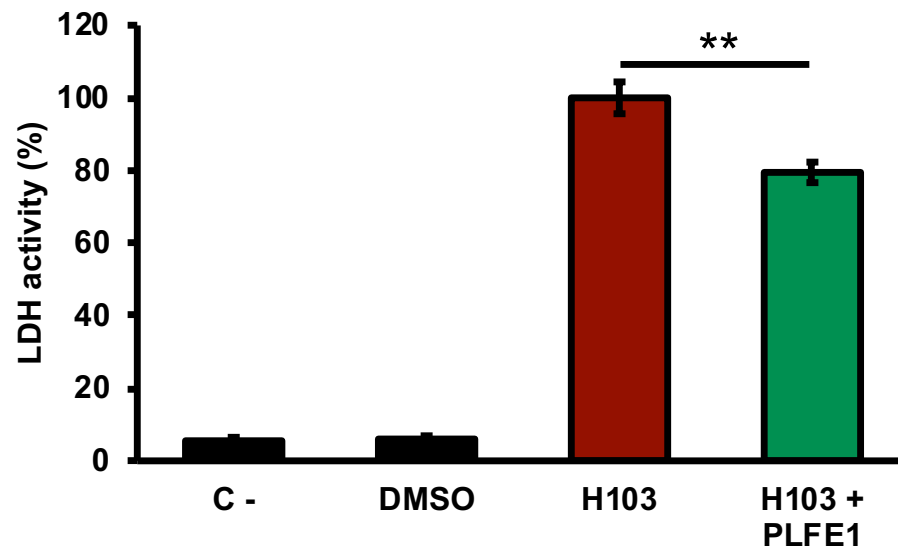




# Figure 2

bioRxiv preprint doi: <https://doi.org/10.1101/2020.03.17.995043>; this version posted March 19, 2020. The copyright holder for this preprint (which was not certified by peer review) is the author/funder. All rights reserved. No reuse allowed without permission.

## A



## B

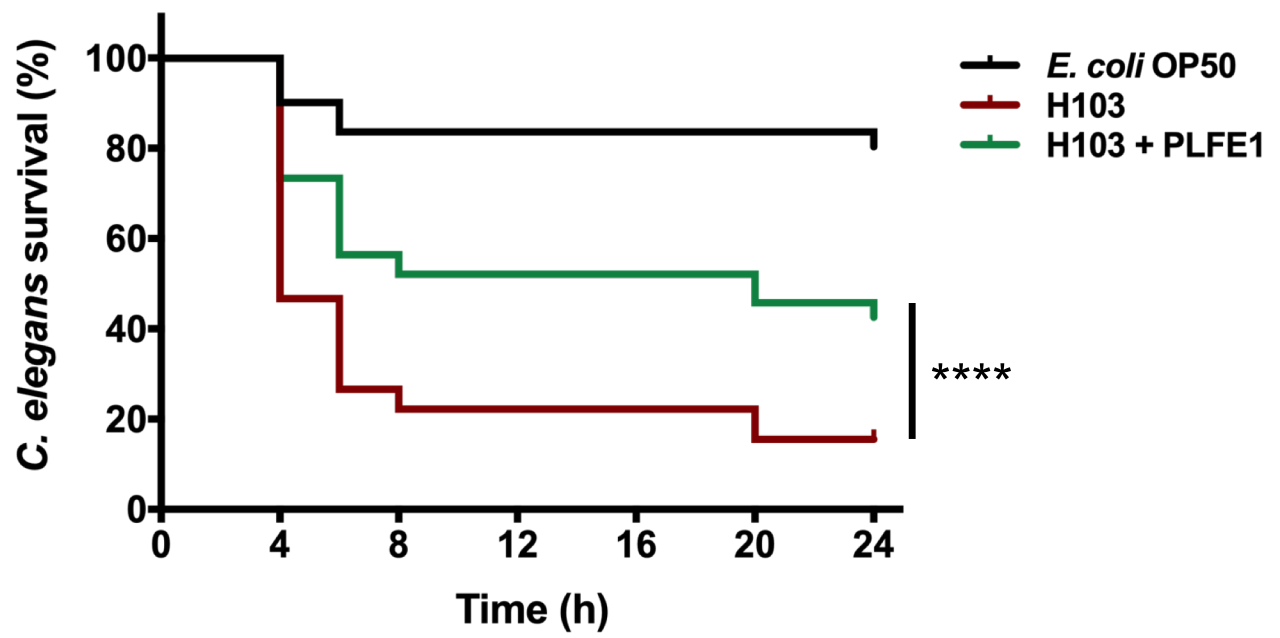
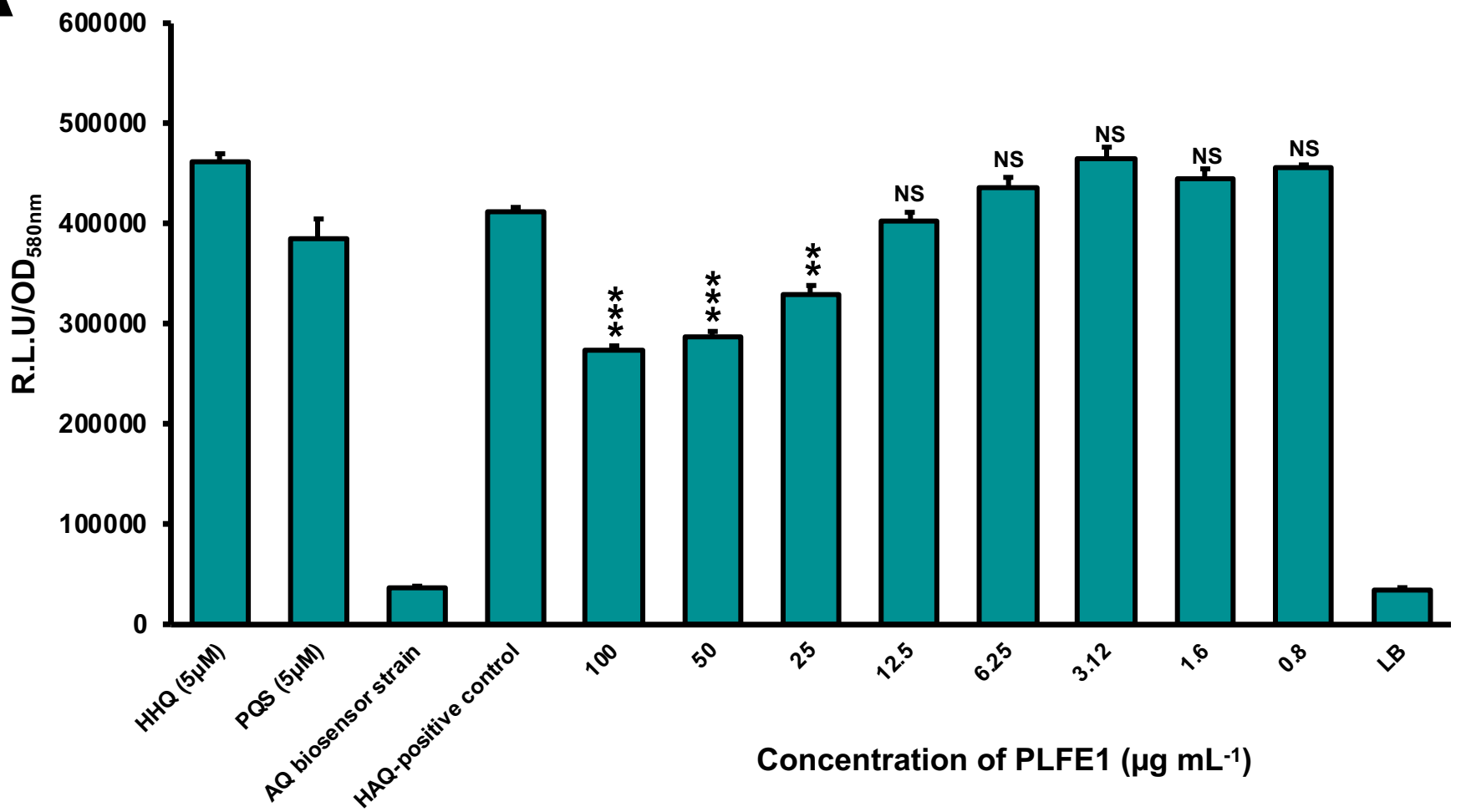


# Figure 3

bioRxiv preprint doi: <https://doi.org/10.1101/2020.03.17.995043>; this version posted March 19, 2020. The copyright holder for this preprint (which was not certified by peer review) is the author/funder. All rights reserved. No reuse allowed without permission.

## A



## B

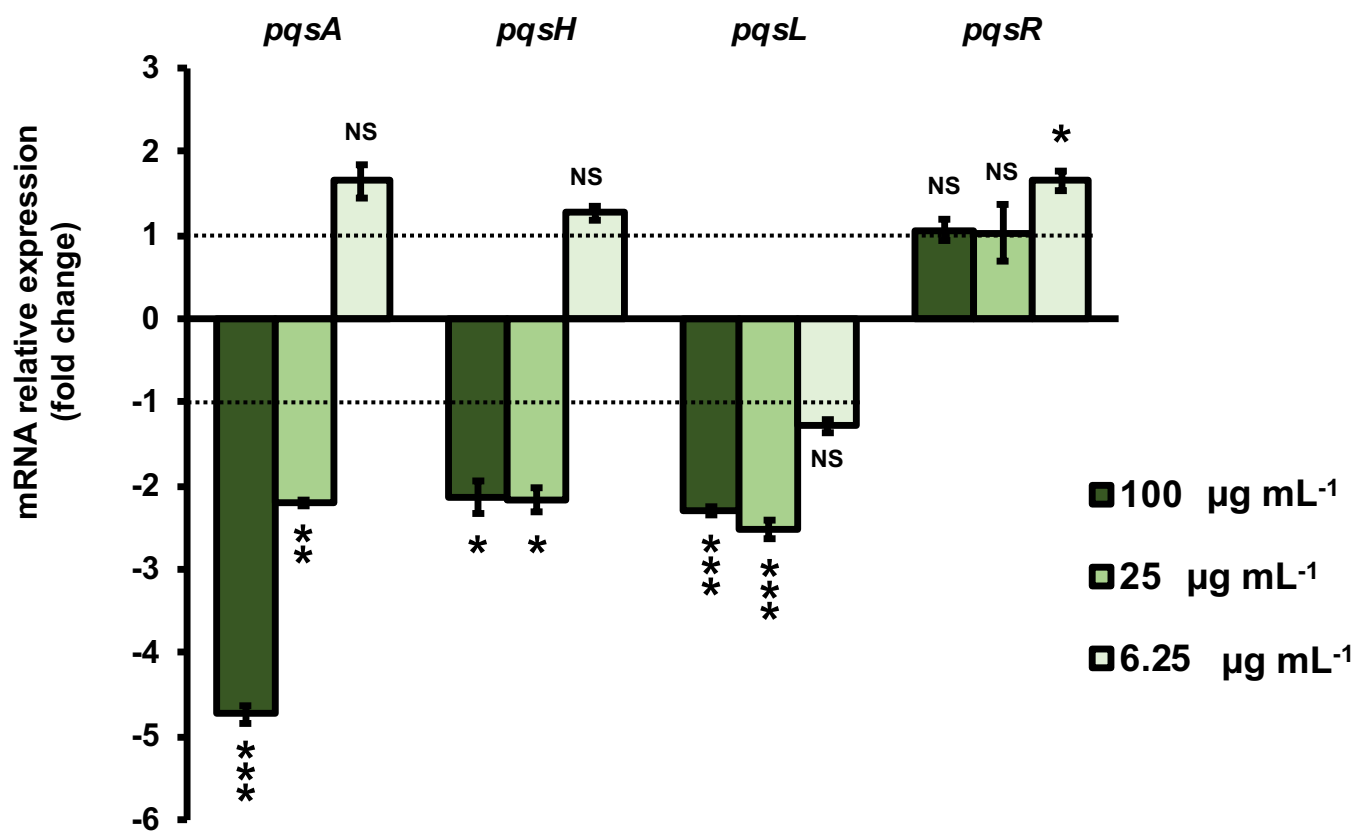
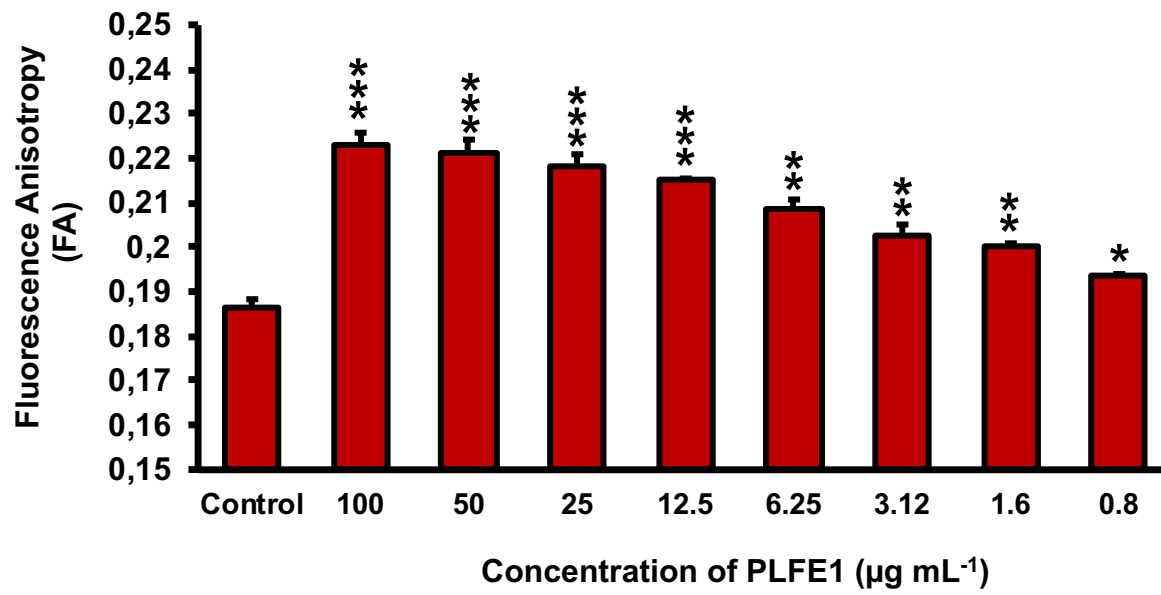


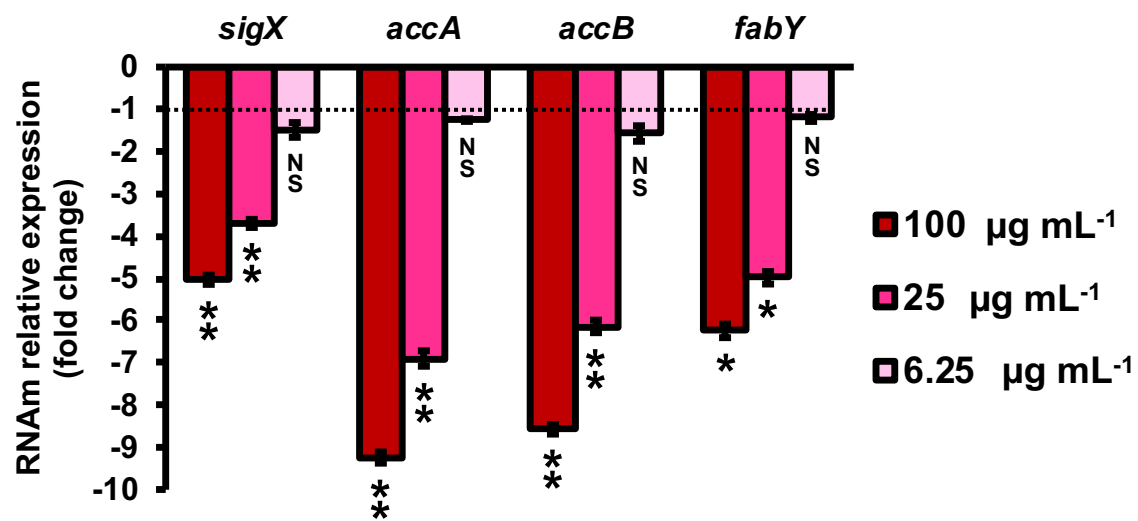
# Figure 4

bioRxiv preprint doi: <https://doi.org/10.1101/2020.03.17.995043>; this version posted March 19, 2020. The copyright holder for this preprint (which was not certified by peer review) is the author/funder. All rights reserved. No reuse allowed without permission.

## A



## B



## C

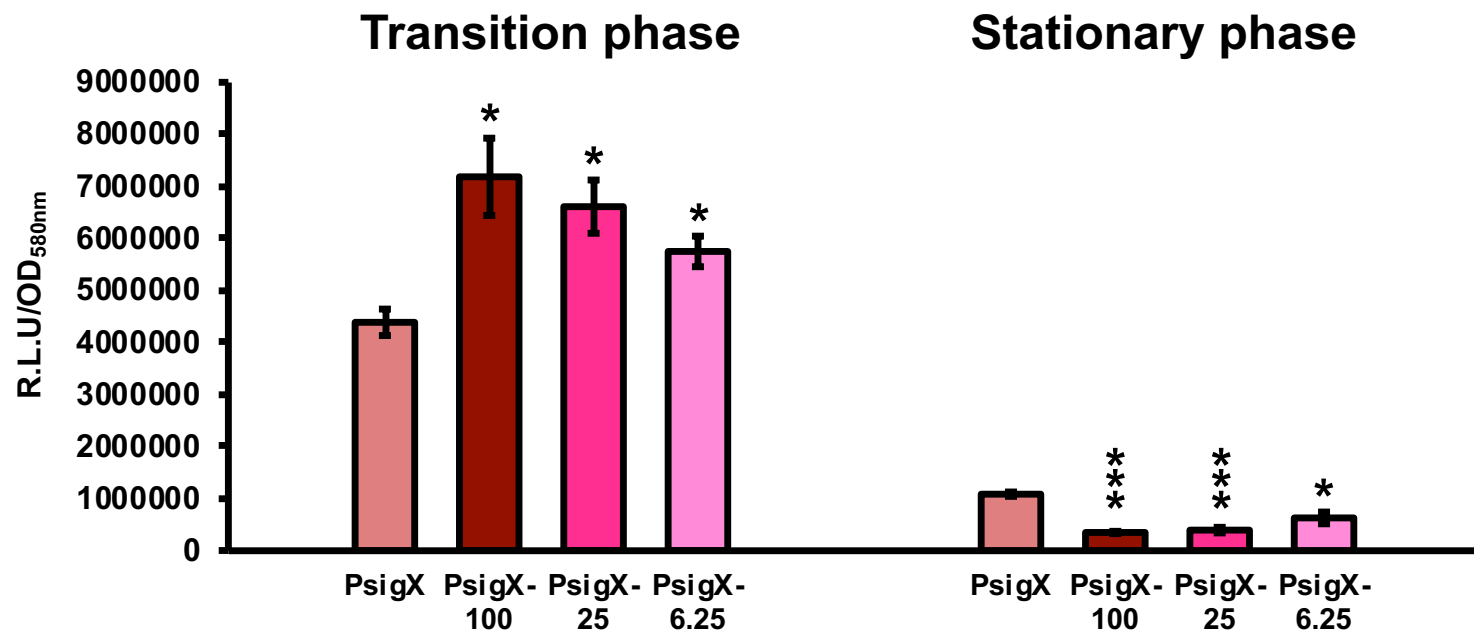


# Figure 5

bioRxiv preprint doi: <https://doi.org/10.1101/2020.03.17.995043>; this version posted March 19, 2020. The copyright holder for this preprint (which was not certified by peer review) is the author/funder. All rights reserved. No reuse allowed without permission.

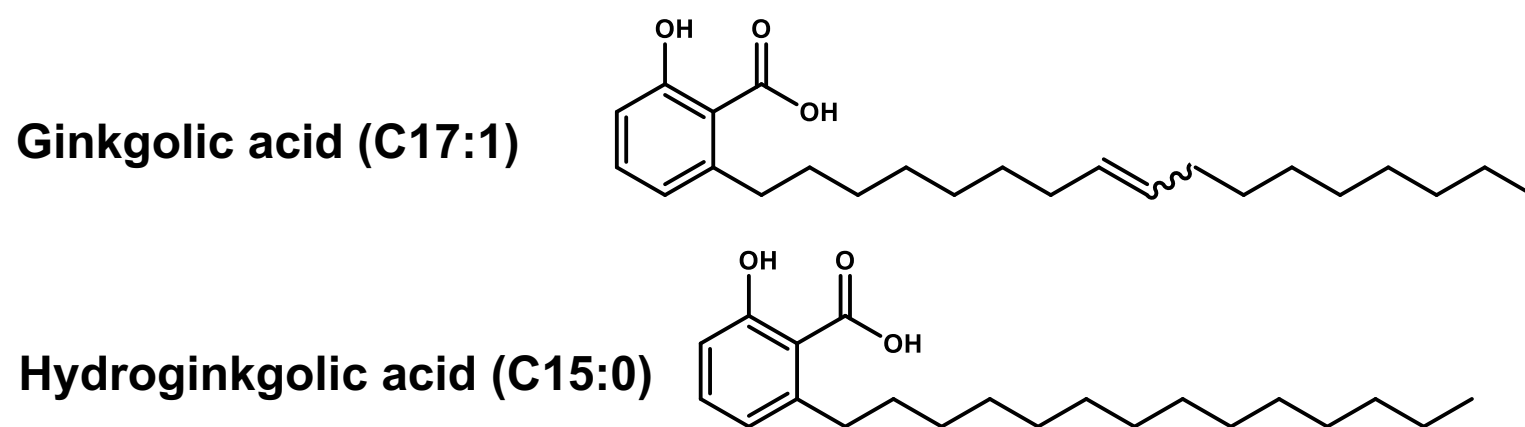
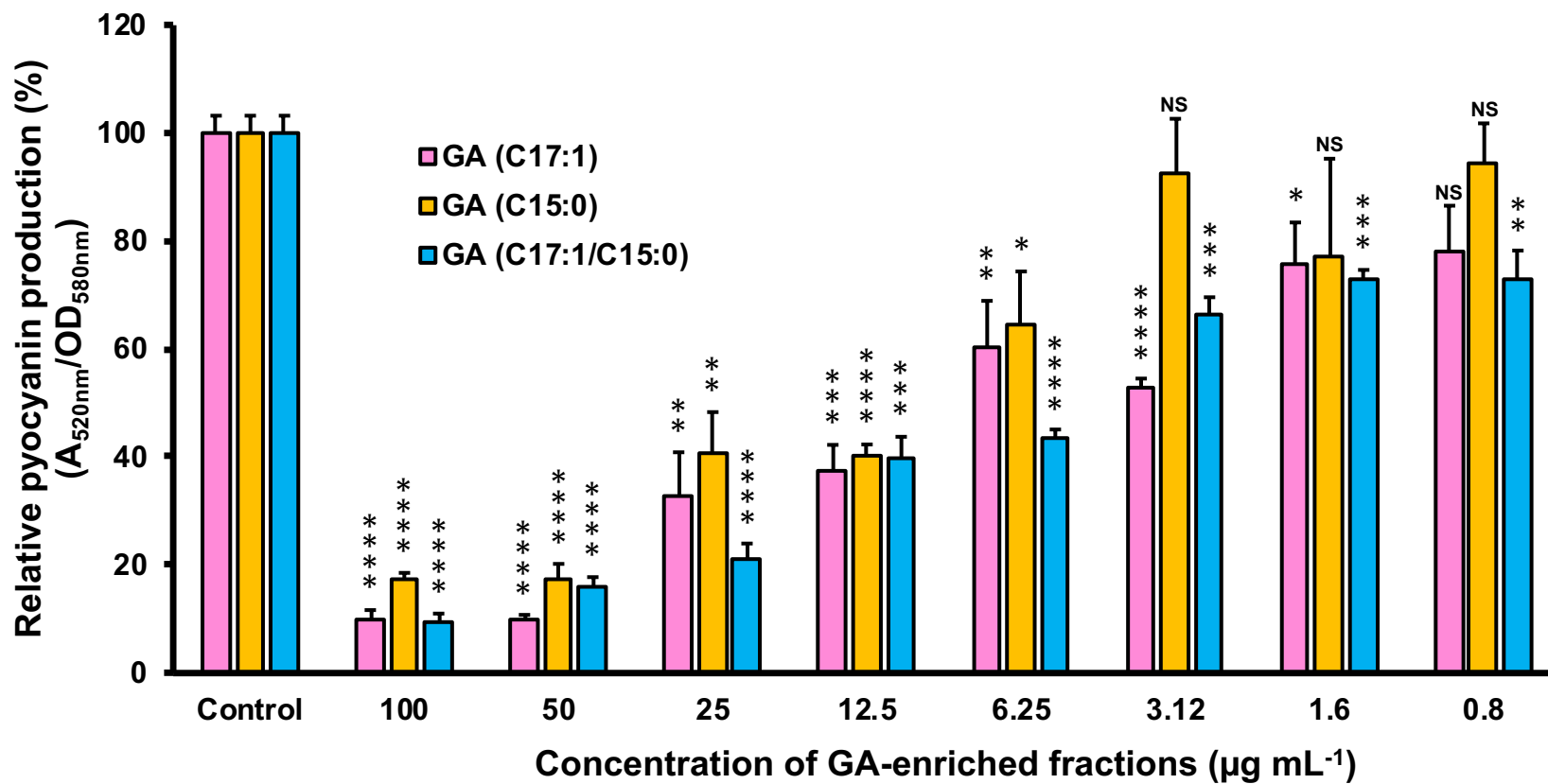


# Figure 6

bioRxiv preprint doi: <https://doi.org/10.1101/2020.03.17.995043>; this version posted March 19, 2020. The copyright holder for this preprint (which was not certified by peer review) is the author/funder. All rights reserved. No reuse allowed without permission.

## A



## B

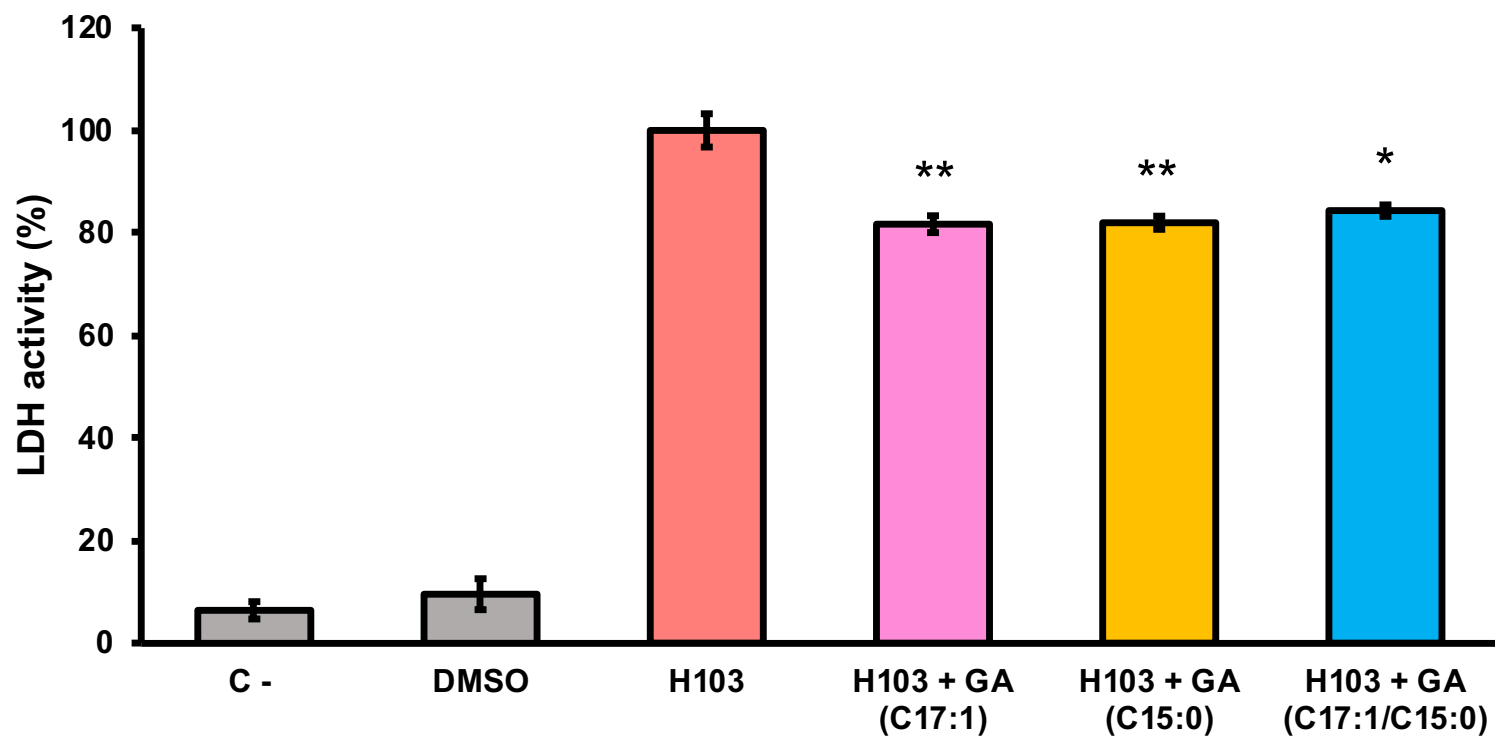
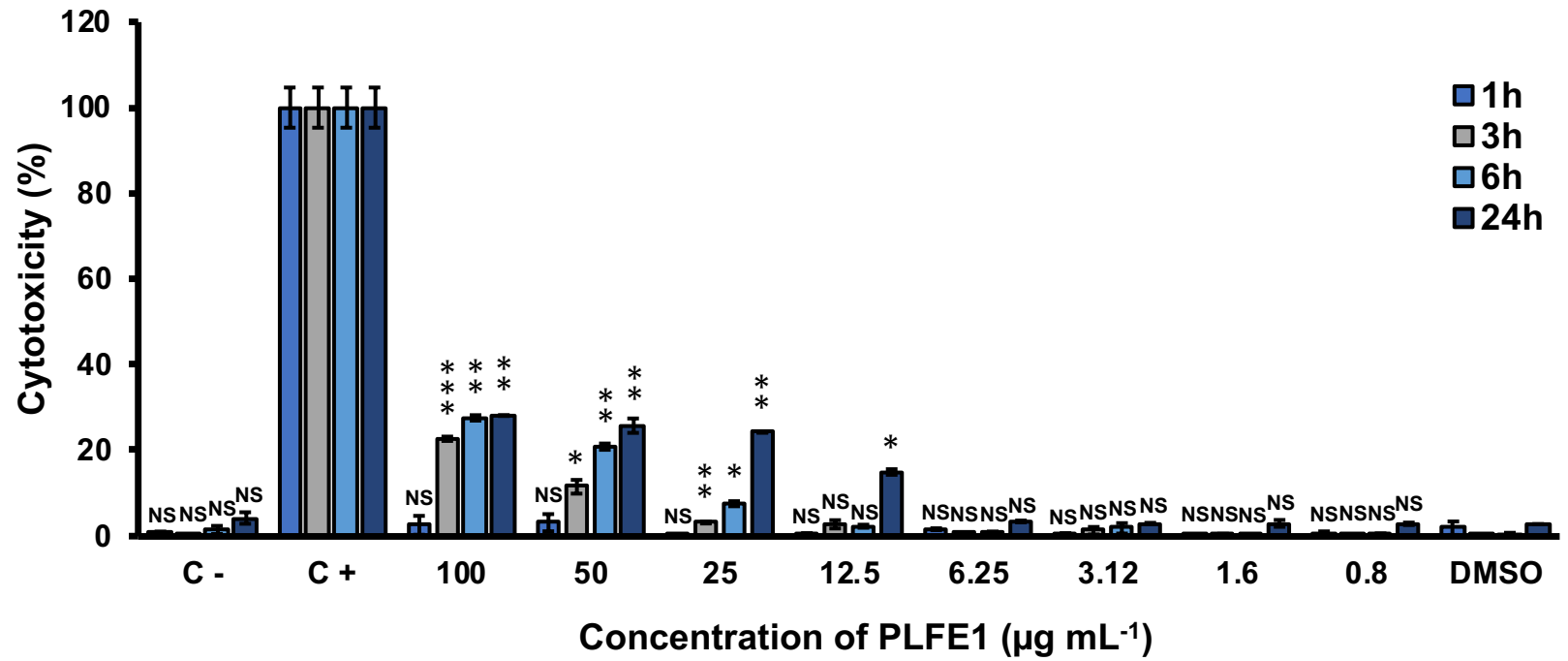


# Figure 7

bioRxiv preprint doi: <https://doi.org/10.1101/2020.03.17.995043>; this version posted March 19, 2020. The copyright holder for this preprint (which was not certified by peer review) is the author/funder. All rights reserved. No reuse allowed without permission.

## A



## B

